USE OF PASSIVE FILTERS TO MINIMISE HARMONICS GENERATED BY SOLAR PHOTOVOLTAIC SYSTEMS AND NON-LINEAR LOADS

By

Sinethemba Neku

Student number:

Submitted in fulfilment of the requirements for the degree:

MASTER OF ENGINEERING:

ELECTRICAL ENGINEERING

In the

Faculty of Engineering and Information Technology:

School of electrical, electronic and Computer Engineering

At the

Central University of Technology, Free State

Supervisor: **Dr Sandile Phillip Koko** (D.Eng: Electrical Engineering)

Bloemfontein

2025

Declaration

I, Sinethemba Neku declare that this research project which has been submitted in fulfilment of the requirements for VHA50AI towards MASTER OF EGINEERING: ELECTRICAL ENGINEERING at Central University of Technology, is my own independent work; it complies with the Code of Academic Integrity, relevant policies, procedures, rules and regulations of Central University of Technology, Free State. This research has not been submitted previously for qualification purposes, where necessary the work and/or ideas of others has clearly been cited and referenced.

Student Signature

Date: 2025-07-14

Acknowledgements

I would like to thank God; through unforeseen circumstances and nature of my professional work, I have managed to successfully complete my research and write this dissertation. I would have not managed to complete without his strength and faith he has given me.

I am deeply grateful to my supervisor, Dr Sandile Phillip Koko, for being patient with me. His continued advice, guidance and support throughout my research has played a crucial role in completing my dissertation.

I would like to thank Mr Sibulele Mtakati for his continued support in my Masters journey.

I am forever thankful to my wife (Sinazo Ntondini-Neku) and my son (Thandoluhle Neku) for unconditional love and support throughout my studies.

Finally, I would like to thank CUT for the opportunity to conduct my research and for the financial assistance they have provided.

Abstract

Solar photovoltaic (PV) technology is increasingly gaining attention in South Africa due to its low maintenance and operating costs, as well as its ability to address power outages. However, both grid-tied solar PV systems and non-linear loads introduce harmonic currents into the grid, which can significantly impact power quality. These harmonics lead to distortions in the voltage and current waveforms of the grid network.

However, regardless of the harmonics introduced into the grid network, a weak grid network can also adversely affect the performance of grid-tied solar PV systems. Many studies have examined the power quality issues of these solar PV systems without accounting for the negative effects of a weak grid-network itself. The strength of a grid network can vary based on the geographical area and the point of common coupling (PCC) where the renewable energy system connects to the grid. The grid's strength is determined by its source impedance, which encompasses all the equipment involved in power transmission, including transmission cables, transformers, and other components.

The purpose of this dissertation is to design and implement four-star branch RCL passive filter that will eliminate harmonics generated by PV grid-tied system and nonlinear loads in a weak or good grid-network. Furthermore, the effects of a weak grid network have been examined to ensure that the designed filter effectively minimizes total harmonic distortion (THD) within the system, because of non-linear load, solar PV and weak grid-network. A power simulation (PSIM) software has been used to model a grid-tied solar PV network supplying nonlinear loads in order to analyse the harmonics, as well as designing the proposed RCL passive filter. Fast Fourier Transform (FFT) and THD functions of the software are used as a baseline parameter to analyse the simulation results.

The study's findings showed that by integrating a weak grid-network with a solar PV system supplying non-linear loads can lead to increased THD in both current and voltage waveforms, compared to a strong grid-network. It is of great significance to analyse the quality of a grid network before designing a passive filter to be used to mitigate the harmonics injected by a power generation system.

In this study, the designed filter has proved to effectively reduce the THD injected by a combination of solar PV system, weak grid-network and non-linear loads, using four branch RLC filter connected to a three-phase four-wire inverter, using PSIM simulator/software. The results showed that the designed filter managed to drastically reduce the %THD of both current and voltage waveforms from 91.5 % to 3.6 % and from 38% to 5.7%, respectively. Under a strong grid-network, the %THD were reduced from 41.7 % to 2.7 % and from 10 % to 3.7 % THD, respectively. For both cases, the minimum allowable limit set by IEEE standards for low voltage system (<1 kV) was met. The designed filter proved to successfully mitigate the harmonics from the worst-case scenario (strong grid-network) to a more favourable one (strong grid-network).

Table of Contents

Declaration ii
Acknowledgements iii
Abstract iv
List of Figures viii
List of Tables x
Abbreviation xi
CHAPTER 1: INTRODUCTION 1
1.1. Background 1
1.2. Problem Statement 2
1.3. Objectives of the Study 3
1.4. Research Methodology 4
1.5. Hypothesis 5
1.6. Limitation of the Study 5
1.7. Contribution to Knowledge 5
1.8. Research Output 6
1.9. Outline of the Dissertation 6
CHAPTER 2: LITERATURE REVIEW 8
2.1. Introduction 8
2.2. Electricity challenges in South Africa 8
2.3. Nature of nonlinear loads 9
2.4. Linear loads 10
2.5. PV Solar System 11
2.6. Understanding power system harmonics 17
2.6.1. Sources of harmonics and harmonic standards 18
2.6.2. Harmonic elimination strategies 19
2.6.3. Effects of harmonics 21
2.7. Impact of source impedance on voltage supply waveforms 22
2.8. Recent studies on use of passive filters to mitigate harmonics in solar PV systems 23
2.8.1. Off-grid solar PV system 23
2.8.2. Grid-connected solar PV system 25
2.9. Conclusion 29

CHAPTER 3: ANALYSIS OF HARMONICS BASED ON LOAD TYPE AND GRID IMPEDANCE 30
3.1 Introduction 30
3.2 Simulation study 30
3.2.1 Linear load on strong grid. 31
3.2.2 Nonlinear load on strong grid. 33
3.2.3 Weak grid supplying nonlinear load 34
3.2.4 Grid-tied Solar PV system with non-linear load 36
3.3 Comparative Summary 44
3.4 Conclusion 44
CHAPTER 4: DESIGN OF FOUR BRANCH RCL HARMONIC PASSIVE FILTER 45
4.1. Introduction 45
4.2. Circuit diagram of the PV grid-tied system with RCL filter 45
4.2.1. Design of a positive-negative sequence single-tuned RCL filter 47
4.2.2. Design of a zero-sequence neutral branch of a RCL filter 50
4.2.3. Frequency domain plot of filter impedance 51
4.3. Simulation circuit 53
4.4. Simulation Results 54
4.4.1. Synchronisation of the inverter with the grid 54
4.4.2. Case 1 Simulation Results: Strong grid-network system (without a filter) 56
4.4.3. Case 1 Simulation Results: Strong grid-network system (with a proposed filter) 59
4.4.4. Case 2 Simulation Results: Weak grid-network system (without a filter) 62
4.4.5. Case 2 Simulation Results: Weak grid-network system (with a filter) 65
CHAPTER 5: CONCLUSION AND FUTURE STUDIES RECOMENDATION 68
REFERENCES 69

List of Figures

Figure 2.1: Distorted current waveforms drawn by nonlinear linear loads [7].....10
Figure 2.2: Ideal current waveform drawn by the linear load [14].....11
Figure 2.3: Different types of PV solar systems [13].....12
Figure 2.4: Grid-tied PV solar system [17].....14
Figure 2.5: Hybrid PV solar system in a residential scale [21].....15
Figure 2.6: Off-grid PV solar system in a residential scale [22].....16
Figure 2.7: Different passive filter topologies used to filter different harmonic orders [7].....20
Figure 2.8: Passive filter topologies used to filter different harmonic orders [9].....21
Figure 2.9: Equipment that makes up source impedance [5].....22

Figure 3.1: Pure resistive load connected directly to AC grid supply.....32
Figure 3.2: Supply current and line voltage simulation results of pure resistive load connected to grid.....32
Figure 3.3: Harmonic spectrum of supply current and supply line voltage of linear load connected to grid.....32
Figure 3.4: Nonlinear load connected to AC grid supply circuit.....33
Figure 3.5: Supply current and line voltage waveforms influenced by a nonlinear load connected to grid.....33
Figure 3.6: Harmonic spectrum of supply current and line voltage as influenced by a nonlinear load.....34
Figure 3.7: A nonlinear load supplied by a weak AC grid-network.....35
Figure 3.8: Voltage and current waveforms as influenced by a weak grid-network.....35
Figure 3.9: Harmonic spectrum of current and voltage waveforms as influenced by a weak grid-network.....36
Figure 3.10: Grid-tied solar PV system supplying a nonlinear load.....37
Figure 3.11: Inverter output current.....38
Figure 3.12: Harmonic spectrum of inverter output current waveforms.....39
Figure 3.13: Inverter output voltage.....39
Figure 3.14: Harmonic spectrum of inverter output voltage waveforms.....40
Figure 3.15: Non-linear load current waveforms for the Grid-tied PV system (strong grid)..41
Figure 3.16: Harmonic spectrum of non-linear load current waveforms.....41
Figure 3.17: Non-linear load voltage waveforms for the Grid-tied PV system (strong grid)..42
Figure 3.18: Harmonic spectrum of non-linear load voltage waveforms.....42
Figure 3.19: Grid current waveforms for Grid-tied PV system with nonlinear load drawing current.....43
Figure 3.20: Harmonic spectrum of load current waveforms for Grid-tied PV system with nonlinear load drawing current.....43

Figure 4.1: Single line circuit diagram of PV grid-tied system with RCL filter.....46

Figure 4. 2: RCL passive filter branch 47
Figure 4. 3 Frequency domain plot of RCL filter impedance 52
Figure 4.5: Grid-tied solar PV simulated circuit diagram with nonlinear load and RLC filter 55
Figure 4.6: hysteresis current controller band 56
Figure 4.7: Grid currents waveforms when filter not connected in a strong network 57
Figure 4.8: Harmonic spectrum of grid current when filter not connected in a strong network 57
Figure 4.9: Grid voltage waveforms when filter not connected in a strong network 58
Figure 4.10: Harmonic spectrum of grid voltage when filter not connected in a strong network 59
Figure 4.11: Grid currents waveforms when the filter is connected in a strong network 60
Figure 4.12: Harmonic spectrum of grid current when filter is connected in a strong network 60
Figure 4.13: Grid voltage waveforms when filter is connected in a strong network 61
Figure 4.14: Harmonic spectrum of grid voltage when filter is connected in a strong network 61
Figure 4.15: Grid currents waveforms when filter not connected in a weak grid-network 63
Figure 4.16: Harmonic spectrum of grid current when filter not connected in a weak network 63
Figure 4.17: Grid voltage waveforms when filter not connected in a weak network 64
Figure 4.18: Harmonic spectrum of grid voltage when filter not connected in a weak network 64
Figure 4.19: Grid currents waveforms when filter is connected in a weak network 65
Figure 4.20: Harmonic spectrum of grid current when filter is connected in a weak network 66
Figure 4.21: Grid voltage waveforms when filter is connected in a weak network 67
Figure 4.22: Harmonic spectrum of grid voltage when filter is connected in a weak network 67

List of Tables

Table 2.1: Ideal Harmonic phase sequence in three phase power systems [21]. 17
Table 2.2:Voltage harmonic limits for low voltage and high voltage on the grid [26] 19
Table 2.3: Current harmonic limits in a power system [26] 19

Table 3.1: Total harmonic distortion (p.u) of supply current and line voltage influenced by a non-linear load 34
Table 3.2: Table showing total harmonic distortion (p.u) results of supply current and voltage influenced by a weak grid-network..... 36
Table 3.3: Total harmonic distortion of inverter output current 39
Table 3.4: Total harmonic distortion of inverter output voltage..... 40
Table 3.5: Total harmonic distortion of load current..... 41
Table 3.6: Total harmonic distortion of non-linear load voltage 42
Table 3.7: Total harmonic distortion of grid current 44
Table 3. 8 Comparative summary of the results 44

Table 4. 1 Impedance vs frequency RCL filter data 52
Table 4.2: Simulated circuit parameters 53
Table 4.3: Total harmonic distortion of grid currents when filter not connected in a strong network 58
Table 4.4: Total harmonic distortion of grid voltage when filter not connected in a strong network 59
Table 4.5: Total harmonic distortion of grid currents when filter is connected in a strong network 66
Table 4.6: Total harmonic distortion of grid voltages when filter is connected in a weak network 67

Abbreviation

AC	Alternating Current
CAN	Controller Area Network
DC	Direct Current
DNP3	Distributed Network Protocol 3
DG	Diesel Generator
ESKOM	Electricity Supply Commission
FFT	Fast Fourier Transform
HVDC	High-Voltage Direct Current
IGBT	Insulated-Gate Bipolar Transistor
IPP	Independent Power Producer
IEC	International Electrotechnical Commission
kVA	Kilo-volt-amperes
LV	Low Voltage
MPPT	Maximum Power Point Tracking
MW	Megawatt
NMD	Notified Maximum Demand
PSIM	Power simulation software
PV	Photovoltaic
PPA	Power Purchase Agreement
PPC	Point of Common Coupling
PWM	Pulse-width modulation
RLC	Resistor Inductor Capacitor
RJ45	Registered Jack-45
RS485	Recommended Standard #485
SSEG	Small Scale Embedded Generator
THD	Total Harmonic Distortion
VSI	Voltage Source Inverter

CHAPTER 1: INTRODUCTION

1.1. Background

South Africa faces a continuous energy crisis due to an imbalance between electricity supply and demand, resulting in frequent power outages that negatively affects economic activities. South Africa relies heavily on coal for energy production (69%), followed by crude oil (14%), renewables (11%), gas (3%), and nuclear (3%) [1]. While Eskom and Independent Power Producers (IPPs) contribute to the energy supply in the country, the current generation capacity remains insufficient.

Globally, an increase in greenhouse gases and growing electricity demand have encouraged the deployment of renewable energy systems as a sustainable and viable means of energy supply. South Africa have signed a Kyoto Protocol and Paris Agreement to reduce greenhouse gas emission level and to accelerate the adoption of renewable energy technologies, particularly sola photovoltaic (PV) systems which are among the cleanest energy sources [2]. Grid-tied solar PV systems allow consumers to offset their energy costs and export excess power to the grid, increasing public interest in rooftop installations [3].

However, integrating solar PV into the grid introduces challenges such as harmonic distortion, especially when nonlinear loads and power electronic converters are involved. These harmonics can degrade power quality, cause voltage fluctuations, and stress utility infrastructure [4].

Grid impedance that is determined by the geographical distance from the power generation sources varies across the regions. High source impedance can induce voltage drops and instability while low impedance may enhance the power flow. Hence, grid impedance in urban and remote areas is not the same [5]. Conductors, transformers, connections, and power devices

are the major factors that determine the utility impedance of the area. A high source impedance is known as a weak grid-network and may negatively affect the total harmonic distortion (THD) in a distributed generation system. Hence, a study needs to be undertaken to evaluate the impact of a weak grid network on THD when integrated with a solar PV system.

The local utility grid companies are given a THD limits and standards to control the harmonics injected into the network by each consumer. According to IEEE 519-1992 standards, the allowable maximum THD limits in system voltages of 1kV or less is 5% for current and 8% for voltage [6]. Harmonics minimization can be achieved by using passive or active filters. Passive filters are designed using passive elements such as resistors, inductors, and capacitors, while active filters are designed using active elements such as transistors and diodes. [7] [8].

Several studies have been conducted to eliminate harmonics generated by solar PV systems and nonlinear load. However, these studies did not take the impact of a utility network impedance into consideration when connected to a grid-tied solar PV system. It is essential to consider the effects of the utility network impedance, as it directly reveals the overall quality of the network itself. Hence, in this study, the impact brought by the weak grid-network coupled to a solar PV system supplying a non-linear load will be investigated to design a passive filter. The passive filter should effectively minimize the THD injected by the combination of solar PV system, weak grid-network, and non-linear loads. This will be achieved by modelling the entire system to analyse the dominant harmonic orders to be eliminated by the designed passive filter.

1.2. Problem Statement

Solar PV systems and nonlinear loads in a three-phase four-wire system, distort the supply current and results in high neutral currents. They reduce electrical equipment lifespan and protection devices lose their sensitivity. Several research studies based on the use of passive

filters to eliminate harmonics in solar PV systems were undertaken. However, because utility impedance varies depending on geographic location, these research did not account for it. This determines the power quality of the network. In remote or rural areas, source impedance tends to be high, primarily due to the distance of the transmission lines and the network equipment used to deliver power from the generation station to rural areas.

Hence, this study proposes a filter designed to effectively reduce the THD injected by a combination of solar PV system, weak grid-network and non-linear loads. The filter performance will be studied under both weak and strong grid network. The RCL (Resistor-Capacitor-Inductor) filter connected to a three-phase four-wire inverter is proposed in this study. The inverter and the grid network will consist of three AC live conductors and the neutral conductor.

1.3. Objectives of the Study

The aim of this research is to propose and design a suitable filter that will eliminate harmonics injected by a combination of solar PV system, weak grid-network, and non-linear loads. The filter will be applicable to small-scale PV solar systems that are not more than 1 MW in size. This will assist in improving the life span of the appliances.

Below are the specific objectives of this research:

I. To further investigate different passive filters literatures aimed to eliminate harmonics in grid-tied solar PV system.
II. To model the grid-connected solar PV system on PSIM, as well as to analyse the dominant harmonic orders to be eliminated when the system is connected to a weak or strong grid-network.
III. To analyse the dominant harmonics in the modelled grid-connected solar PV system.

IV. To propose and design a passive RLC filter that will effectively reduce the total harmonic distortion in both current and voltage waveforms of the proposed grid-connected solar PV system.

V. To present the findings of the study in the detailed report.

1.4. Research Methodology

This methodology outlines the process to achieve the research objectives:

I. **Literature survey:** A comprehensive survey of different literatures that use passive filters to eliminate harmonics in grid-tied solar PV systems will be carried out. The findings will be discussed and the gaps not covered by these studies will be highlighted.

II. **System modelling and simulation:** A grid-connected PV solar system will be modelled using the PSIM software package. The simulations will be carried out to analyse the impact of non-linear loads in the modelled solar PV system connected to a weak and to a strong grid-network. The influence of non-linear loads and grid-network impedance will be identified.

III. **Harmonic analysis:** Analyse the dominant harmonics in the modelled grid-connected solar PV system supplying non-linear load. The dominant harmonics will be analysed under both strong and weak grid-network cases through Fast Fourier Transform (FFT) to determine the %THD in both current and voltage waveforms.

IV. **Filter design:** A passive RLC filter will be analytically designed using classical filter design equations. Design parameters will be tailored based on the dominant harmonic orders observed. The filter's effectiveness will be validated by comparing pre- and post-filter THD values.

V. **Dissertation writing:** The results of the study will be included in the dissertation, presented at the conference and published in the journal.

1.5. Hypothesis

1. Total harmonic distortion will be reduced using the designed passive filter for a grid-tied solar PV system connected to either a weak or strong grid-network.
2. The filter will ensure THD levels remain within IEEE 519-1992 standards—specifically, below 5% for current and below 8% for voltage in systems rated at 1kV or less.
3. The expected lifespan of the load appliances will be preserved, and the likelihood of conductor burns, and unexpected trips of protection devices will be reduced.

1.6. Limitation of the Study

1. Solar PV system with energy storage systems will not be covered in the study.
2. The inverter and the grid network will be modelled as a three-phase system with a line voltage of 400Vac since single-phase will not be considered in this study.

1.7. Contribution to Knowledge

This study will be published to increase awareness among researchers about the impact of a weak grid network on a solar PV system supplying non-linear loads. While passive filters are a well-established solution for harmonic mitigation, this research introduces a novel dimension by quantifying their performance under varying grid strengths. The study offers a systematic approach to evaluating the impact of utility source impedance on THD and proposes a filter solution robust across both weak and strong grid conditions. The findings can guide filter sizing strategies tailored to geographical grid profiles and improve reliability in distributed energy

systems. It aims to fill the gap in previous research that overlooked the influence of utility grid impedance on THD.

1.8. Research Output

Published Papers:

Neku S, Koko SP, “Impact of a Weak Grid-network on a Grid-tied Solar Photovoltaic System Supplying a Non-linear Load”. In 2023 International Conference on Electrical, Communication and Computer Engineering (ICECCE) (pp. 1-6). IEEE, 29-31 December 2023.

Neku S, Koko SP, “A Four-Branch RLC Filter for a Grid-Tied Solar Photovoltaic System Coupled to a Weak Grid Network.” In 2025 15th International Renewable Energy Congress (IREC), (pp. 1-6). IEEE, 02-04 February 2025.

Neku S, Koko SP, “A Recent Review of Passive Filters as Used in Solar Photovoltaic-Based Systems to Mitigate Harmonics.” In 2025 15th International Renewable Energy Congress (IREC), (pp. 1-6). IEEE, 02-04 February 2025.

1.9. Outline of the Dissertation

Chapter 1: This chapter covers introduction of the dissertation. It presents background, problem statement, research objectives, methodology that will be conducted to complete the study, hypothesis, and research outputs.

Chapter 2: This chapter will consist of a network study. The circuits to be discussed in this research will be simulated and investigated, and different circuit scenarios will be considered. A scenario of a linear load (pure resistive) connected to a grid with no solar PV system on the network will be simulated, and all power quality parameters such as voltage waveforms, current waveforms and frequency will be analysed. Similarly, the network will be modelled where the PV system is connected to the grid with source impedance not ignored while supplying non-

linear loads. The simulations will give evidence of network behaviour towards harmonic generation when the PV system is connected to the grid, supplying non-linear loads

Chapter 3: This chapter will consist of network study. The circuits to be discussed on this research will be simulated and investigated in this chapter. Different scenarios of the circuits will be considered on this chapter, a scenario of a linear load (pure resistive) connected to a grid with no PV solar system on the network will be simulated and all power quality parameters such as voltage waveforms, current waveforms and frequency will be analysed. Similarly, the network will be modelled where PV system is connected to the grid with source impedance not ignored supplying nonlinear loads. The simulations will give evidence of network behaviour towards harmonic generation when PV system is connected to grid, supplying nonlinear loads.

Chapter 4: This chapter will cover the actual design of the harmonic filter. It will elaborate on the formulas to be used and cover all the derivations of each formula. A brief explanation will be given of the specific type of harmonic filter to be used and its benefits compared to other filters. Equivalent circuits of the network and line diagrams of the filter to be designed will be presented. The effectiveness of the four-branch star passive filter will also be discussed. Comparisons of the results will be drawn between when the filter is not installed and when the filter is present.

Chapter 5: Study conclusion and future recommendations will be covered in this chapter.

CHAPTER 2: LITERATURE REVIEW

2.1. Introduction

This chapter critically reviews the current challenges in South Africa's electricity system, the role of nonlinear loads in power quality deterioration, and the characteristics of different solar PV system configurations. A strong emphasis is placed on the sources and effects of power system harmonics and the methodologies used in passive filter design. The section concludes with a critical comparison of recent studies involving the use of passive filters in both standalone and grid-connected solar PV systems, identifying methodological gaps and synthesizing key findings.

2.2. Electricity challenges in South Africa

South Africa is currently facing a significant energy crisis driven by frequent grid outages and rising electricity prices. Hence, South African consumers are not encouraged to rely solely from grid power as a prime source energy. There is a need for alternative power supplies such as renewable energy systems to act as a backup and reduce electricity bills. Solar PV system is one of the best technologies to be used due to its low maintenance and operation cost as well as the high solar radiation level available in South Africa. However, integrating solar PV systems into the existing grid presents power quality concerns, especially with regard to harmonic pollution caused by inverter-based and nonlinear loads.

If the harmonics are not maintained within the IEEE allowable standards, they could have a huge negative impact on the sensitive equipment in the grid network which includes protection equipment such as relays, which might take unrealistic values and lose their sensitivity.

2.3. Nature of nonlinear loads

Non-linear loads are defined as loads that require power conversion from the AC supply for them to operate at maximum capability. Non-linear loads are loads that vary in impedance when sinusoidal voltage is applied. The supplied sinusoidal voltage results in non-sinusoidal flow of current [9]. It is expected that 10 years from now, more than 60% of the load connected to the grid will be non-linear loads; the estimated non-linear load growth includes the residential sector's appliances. AC from the grid is converted to DC for these loads to operate. These loads include computers, printers, TVs, microwaves, etc. Non-linear loads are harmonic-producing loads; they can affect sensitive loads connected to the network if there is high distortion on the voltage waveforms. Generally, the grid-network is designed to operate closely to sinusoidal voltage and current with constant frequency. The local grid codes and standards determine the magnitude of the network voltage and frequency; all appliances and machinery are designed based on the local network standards where they will be operating. The severity of the voltage distortion because of harmonic-producing loads is based on the source impedance and the amount of harmonic current injected into the network [10].

Several types of non-linear loads can be found in the residential and the commercial sector. A high percentage of these non-linear loads are essential to human beings and to the economic growth of the country. Companies in the commercial space use large machines to keep production running, offices use computers to keep their businesses operating and residents use appliances in their daily lives. Most of these loads draw dirty power from the network and continue to make it dirtier due to the load's power conversion for it to operate; such loads are called non-linear loads.

Examples of non-linear loads in the residential sector include TVs, monitors, battery chargers, fans with electronic regulators, air conditioners, refrigerators, washing machines, adjustable

speed drivers, etc. [10]. Examples of non-linear loads in the commercial and industrial sectors include cycloconverters, arc furnaces, switching mode power supplies, chopper circuits, silicon-controlled rectifiers, computers, copy machines, etc. [9]. The distorted current waveforms drawn by non-linear linear loads are shown in Figure 2.1 below.

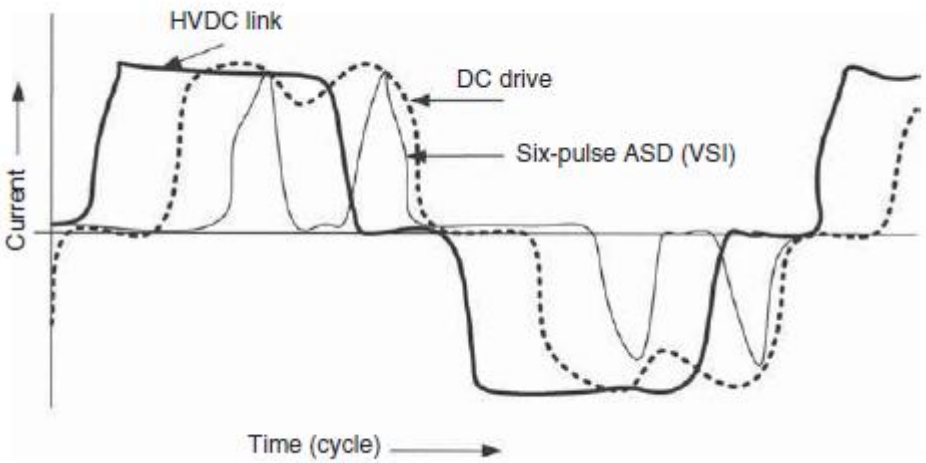

Figure 2.1: Distorted current waveforms drawn by nonlinear linear loads [7].

2.4. Nature of linear loads

Linear loads are described as types of loads that do not produce harmonic distortion to the network when powered or connected to the network. The linear loads, when supplied by a sinusoidal source at the fundamental frequency, produce fair sinusoidal current without distorting the network voltage and current waveforms [11].

Examples of linear loads include induction motors, synchronous motors, power factor improvement capacitors, incandescent lamps, heaters, etc. [9]. The load current does not contain harmonics and, at any given time, is proportional to the voltage [11]. Figure 2.2 shows the current waveform drawn by the linear load. In a balanced three-phase network, the neutral current is zero [12].

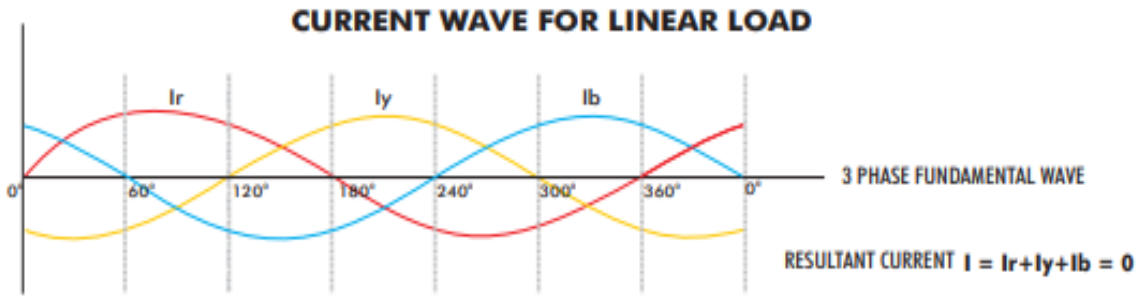

Figure 2.2: Ideal current waveform drawn by the linear load [14]

2.5. PV Solar System

The PV solar system is the type of technology used to generate power; it simply converts sunlight into usable electricity. Irradiance from the sun is directed to the solar panel cells, and solar panels start to generate DC power. The amount of DC power generated by the solar panels depends on many factors: weather conditions (rain, cloud cover, etc.), shading or the angle of the panels facing the sun. In good weather, with solar panels facing north in the southern hemisphere, the solar panel will generate power at its optimum operation [13].

The DC power is then transported to a charge controller or maximum power point tracker (MPPT) and thereafter transported to an inverter where DC power is converted to usable AC power. The AC power can be transported to the grid network, storage system or directly to the load depending on the PV system configuration or power demand. SSEG application is done first before commencing with the solar installation. This is to protect the grid network and ensure the solar plant will abide by the local grid standards and regulations. In the SSEG application, a grid study is conducted where the size of the solar system to be installed is checked, the power factor of the system, acceptable harmonics that can be pushed to the grid, frequency, voltage, and other power quality standards. Once the SSEG application has been

approved, the municipality or power supplier issues a letter of approval for the installation to commence.

The PV solar system consists of various components; these include the solar panel mounting structure, solar panels, rated DC cables, DC cable trays, DC fuses, DC surge protectors, rated DC isolators, charge controllers, MPPT, inverters, AC cables, AC cable ladders, motorized circuit breakers, batteries, AC isolators and communication devices for monitoring the plant. There are three main configurations of the PV system: off-grid system, grid-tied system, and hybrid system. The different PV solar systems with or without battery storage are represented in Figure 2.3 below [13].

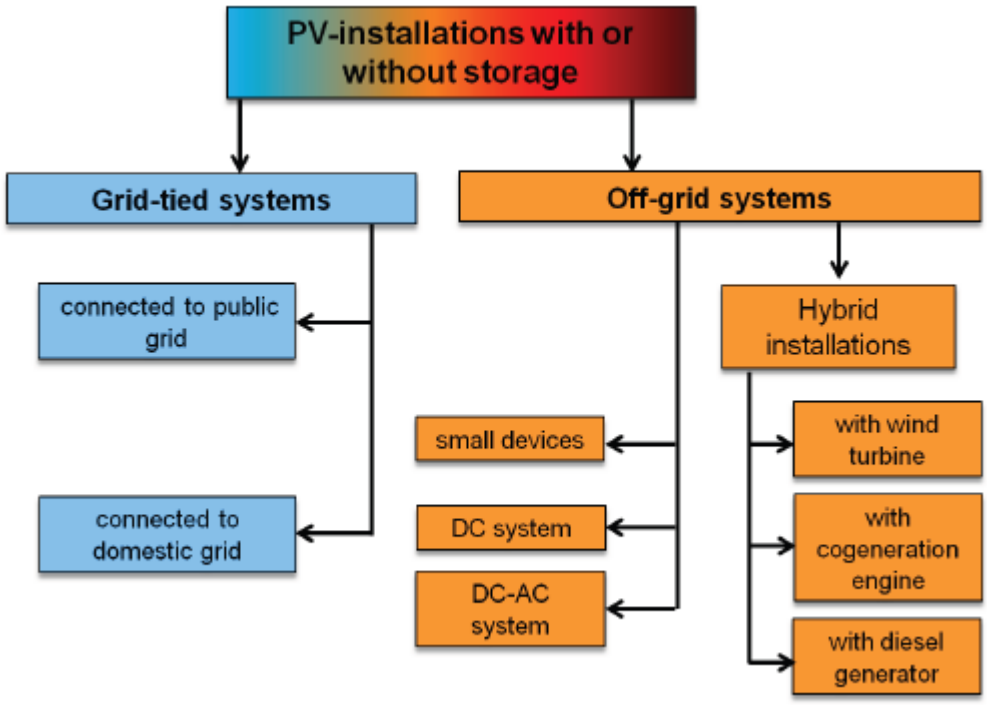

Figure 2.3: Different types of PV solar systems *[13]*

A client with an approved SSEG application has a privilege to feed excess power back to the grid. A client with some shared LV feeders from the supplier has generation limit of 25% of their NMD capacity, this is allowed up to maximum of 20 kVA. Any generator greater than

20 kVA must have its own dedicated feeder [14]. In commercial scale solar plant with PPA contract, the IPP sells power to the utility owner based on agreed tariffs. There is also an option of wheeling when the wheeling contract is in place. Wheeling is whereby the generated power by a private operator in one location is being sold is being sold to a buyer on different location through third party's network [15]

2.5.1. Grid-tied PV solar system

The grid-tied solar system is a solar system that does not have battery storage installed. The inverters convert DC power from the solar panels directly to the grid and load of the network. The inverters need to meet certain power quality requirements that must be approved by the municipality or power supplier for installation. The most critical functionality checked on the inverters is the ability of the inverter to anti-island. This means that when there is a power outage on the grid for whatever reason, the inverter must not export power to the grid. The anti-islanding functionality is done by the contactor inside the inverter, software limiting parameters and the two ABB motorized breakers with an ABB relay.

The grid-tied PV system sizes range from small-scale residential 5 kW up to more than 100 MW commercial plants. The system can be installed on the roof (roof mount), on the ground (ground mount), in car parking areas (carport) or in dams (floating system). The communication and monitoring of the system vary based on the type of technology used by the inverter, but standard communication protocols like RS485, RJ45, CAN, and DNP3 are used. The grid-tied system only produces power during the day. When the solar plant produces more power than required by the load, the excess power is exported to the grid through a bidirectional meter. The bidirectional meter runs backwards to credit the customer account, which is supported by a net-metering policy. When the solar plant produces less power than demanded

by the load, power is imported from the grid to meet the demand [16]. A grid-tied PV solar system is shown in Figure 2.4 below [17].

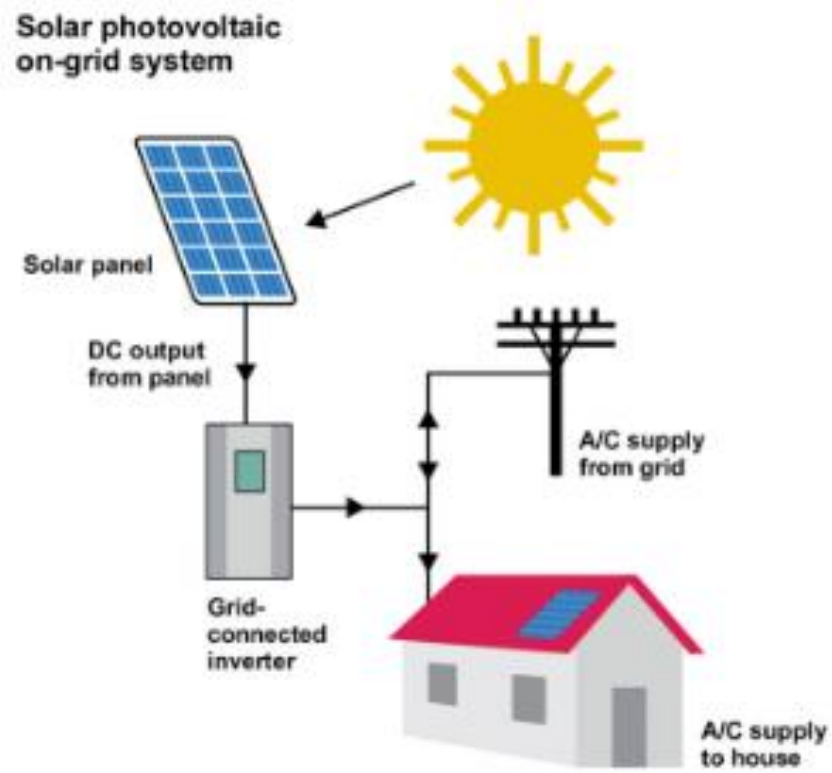

Figure 2.4: Grid-tied PV solar system *[17]*

2.5.2. Hybrid PV solar system

A hybrid PV solar system consists of solar panels, batteries for storage, and a grid connected via the inverter. The generated power is fed to the load and to the utility grid, with the inverter having the capability to anti-island when the grid is not available [18]. This kind of system has an intelligence and algorithm that enables it to switch between using solar power, battery storage or grid power. The batteries can be charged by the solar panels and the grid when the batteries are below the desired state of charge. The main objective of this kind of system is to minimise using grid power and to reduce monthly electricity bills. The hybrid system consists of other installation equipment such as a PV solar module mounting structure, AC and DC

cables, string combiner boxes, AC distribution box, DC and AC surge protective devices, earthing, metering system, monitoring system, etc. [18]. Grid compliance and IP rating of each piece of equipment/device must be carefully considered when selecting or sizing the equipment for the installation. Figure 2.5 demonstrates a hybrid PV solar system on a residential scale [19].

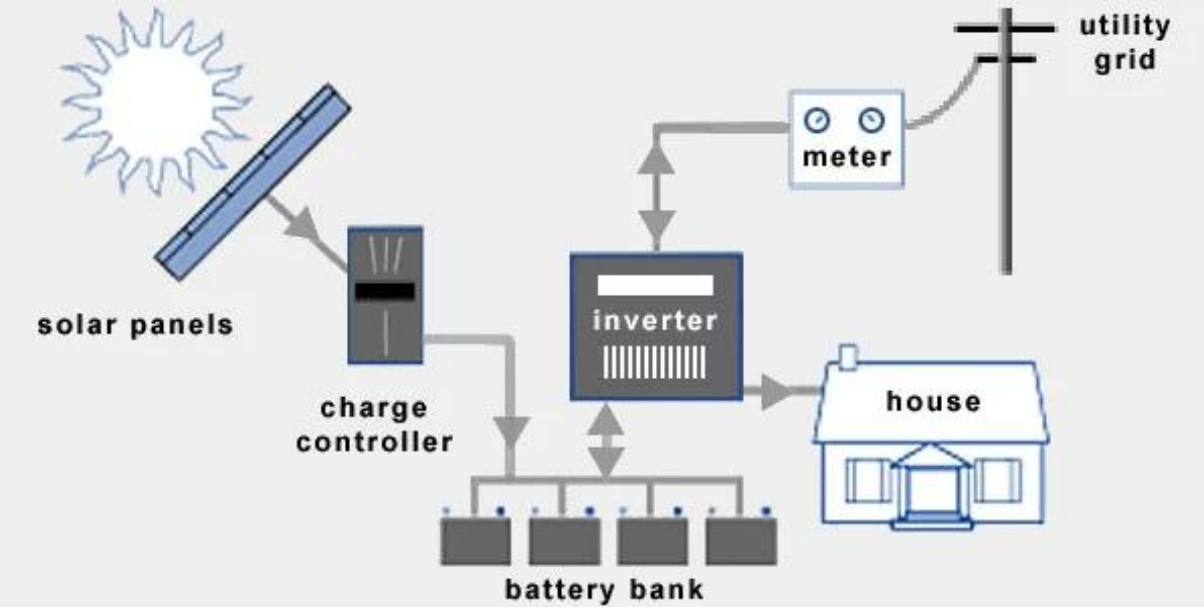

Figure 2.5: Hybrid PV solar system in a residential scale [21].

2.5.2.1. Off-grid PV solar system

An off-grid solar system is a stand-alone solar system that is not fully connected to the grid. Storage equipment, such as the batteries, are the critical components of this kind of system. The batteries of the system can either be charged by the solar panels or by a generator when the state of charge of the batteries is too low and solar panels are not producing enough power to charge the batteries; the batteries can also be charged by solar panels and the generator simultaneously [13]. When designing an off-grid solar system, the load behaviour and autonomy ratio take priority. The autonomy ratio refers to the duration the batteries can supply the load without charging the batteries, this gives an indication of the duration that the batteries

can last on bad weather days without being charged [13]. To obtain a high autonomy ratio and high own consumption ratio, the PV system and batteries must be sized precisely and enlarged.

The off-grid PV system consists of PV solar modules, inverter, batteries, diesel generator, PV solar module mounting structure, AC and DC cables, string combiner boxes, AC distribution box, DC and AC surge protective devices, monitoring system, etc. The size of the system is dependent on the solar user's load profile. The technology and type of equipment to be selected for an off-grid installation depends on the project budget. For a well-designed off-grid system, a diesel generator that can power the loads without the help of solar is advisable. This assists during solar system failure; the system can run in bypass mode and allow the generator to power the loads. Figure 2.6 demonstrates off-grid PV solar system on a residential scale [20].

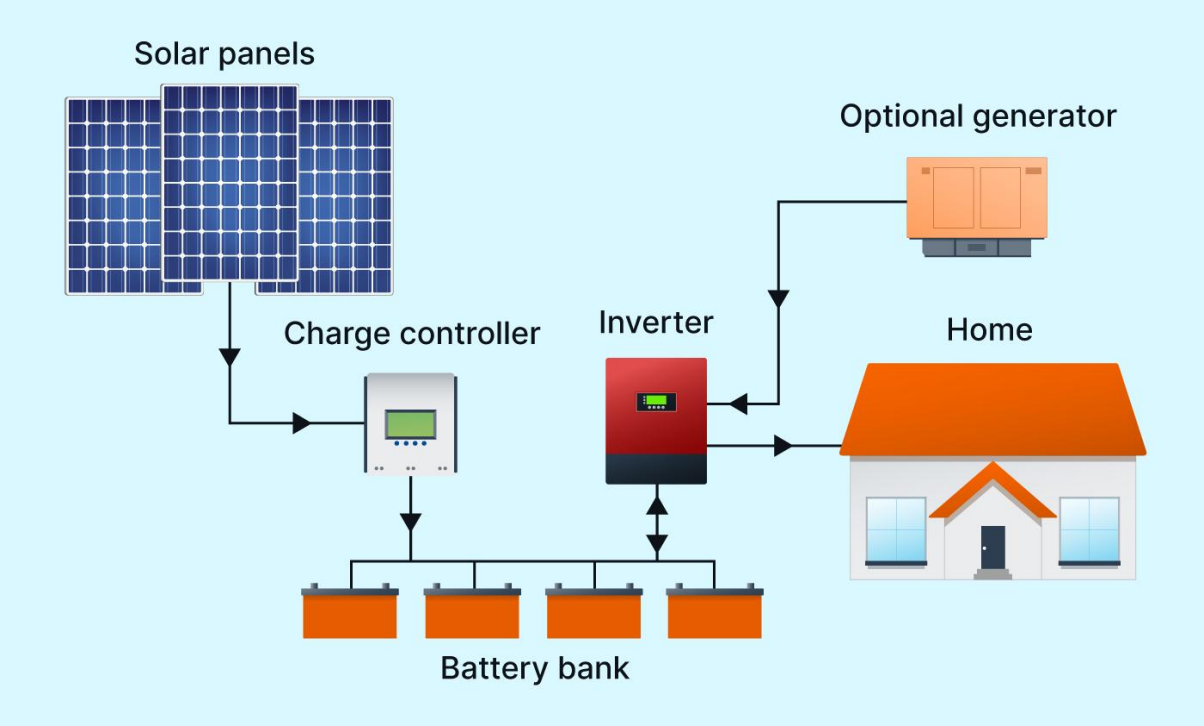

Figure 2.6: Off-grid PV solar system in a residential scale [22].

2.6. Understanding power system harmonics

Power systems and electrical machinery are designed to operate at frequencies of 50 Hz or 60 Hz with pure sinusoidal waveforms of voltage and current. However, certain types of loads such as nonlinear loads produce currents and voltages with frequencies that are integer multiples of the fundamental frequency (50 or 60 Hz). These higher frequencies which are integer multiples of fundamental frequency are known as power system harmonics, they pollute the network and distort the system waveforms [21]. Power system harmonics are a steady-state problem that produce continuous distortion of voltage and current waveforms, harmonics are worse than transient events such as lightning or voltage sags that lasts few microseconds [21]. Fourier analysis is used to present non-sinusoidal waveforms in one graphical periodic waveform with all the harmonic orders present, the highest harmonic interest is normally 25th multiple harmonic order. The total harmonic distortion (THD) is the measure used to measure how distorted the current and voltage waveforms are on the power system [21]. Table 2.1 shows the ideal harmonic phase sequence in a balanced three phase power system [21].

Table 2.1: Ideal Harmonic phase sequence in three phase power systems *[21]*.

Harmonic	Phase sequence
1	+
2	-
3	0
4	+
5	-
6	0
…	…

It should be noted that the harmonic multiples of three are zero sequence harmonic order. They result in being trapped on the neutral conductor. In a balanced three-phase, four-wire network, negative and positive harmonic orders sum up to zero on the neutral conductor, zero sequence orders are the only present harmonic orders on the neutral conductor since they are in phase

with each other [22]. There are equations used to denote positive, negative and zero sequence harmonic orders. Positive is given by I1 = 6k + 1, negative given by I2 = 6k + 5 and zero given by i0 = 6k + 3, where I is the harmonic order and k = 0, 1, 2, 3… [22].

2.6.1. Sources of harmonics and harmonic standards

There are several sources of power systems harmonics. The major source of harmonics is non-linear loads, but conventional power equipment, such as transformers, motors, and generators, generates harmonics under normal operation and by switching transients. The sources of power systems harmonics are divided into two categories: saturable devices and power electronic devices [23]. The common harmonic current sources include power electronic converters, arc furnaces, static VAR systems, inverters, AC phase controllers, cycloconverters, AC-DC converters, and pulse width modulated (PWM) motor drives [24]. Harmonics in transformers are due to the residual or trapped influx after a severe fault, switching, high influx densities, winding connection, or grounding [9]. Power capacitors and transmission lines also contribute to the harmonics of the system. The power electronic circuits for non-linear loads that convert power from AC/DC or DC/AC generate a major percentage of harmonics to the network.

The local power supply or grid owner has harmonic limits and standards that they issue to their customers. This helps the grid owner control the number of harmonics injected by each customer into the grid, and it enables the grid owner to maintain power quality standards. These limits apply at a point of common coupling (PPC) between the grid owner and the customer. Tables 2.2 and 2.3 show voltage harmonic limits for different voltage ranges and current harmonic limits in power systems that all consumers must abide by [24].

Table 2.2:Voltage harmonic limits for low voltage and high voltage on the grid [26]

Bus Voltage V at PCC	Individual harmonic (%)	Total harmonic distortion THD (%)
V≤1.0 kV	5.0	8.0
1 kV≤ V ≤ 69 kV	3.0	5.0
69 kV ≤ V ≤ 161 kV	1.5	2.5
161 kV < V	1.0	1.5

Table 2.3: Current harmonic limits in a power system [26]

Maximum harmonic current distortion in percent of I_L						
Individual harmonic order (odd harmonics) [a, b]						
I_{SC}/I_L	3≤ h <11	11≤ h <17	17≤ h <23	23≤ h <35	35≤ h <50	TDD
<20[c]	4.0	2.0	1.5	0.6	0.3	5.0
20<50	7.0	3.5	2.5	1.0	0.5	8.0
50<100	10.0	4.5	4.0	1.5	0.7	12.0
100<1000	12.0	5.5	5.0	2.0	1.0	15.0
>1000	15.0	7.0	6.0	2.5	1.4	20.0

[a] Even harmonics are limited to 25% of the odd harmonic limits above.

[b] Current distortions that result in a dc offset, e.g., half-wave converters are not allowed.

[c] All power generation equipment is limited to these values of current distortion regardless of actual I_{SC}/I_L, where:

I_{SC} = maximum short-circuit current at PCC

I_L = Maximum demand load current (fundamental frequency component) at the PCC under normal load operating conditions

2.6.2. Harmonic elimination strategies

Harmonics minimisation in solar PV-based systems is achieved using power filters, such as passive or active filters. Passive filters are designed by using passive elements such as resistors, inductors, and capacitors, while active filters are designed by using active elements such as transistors and diodes. Passive filters have proved to be the main choice due to being the most economical and high-performing filters [6] [7]. Passive filters provide low impedance paths for harmonics and enable the harmonics to flow through the filter while preventing the harmonic orders from flowing to the grid [23]. The passive filter can be designed or tuned for single harmonic order or broadband harmonic orders. It all depends on the requirements for the filter

to be installed. The filter is positioned close to the harmonic generators to capture harmonics at the source and confine them to the point of common coupling (PCC), thereby protecting the grid and reducing harmonic emissions at the source.

Different harmonic passive filter topologies can be installed on each phase: low-pass filters, band-pass filters, high-pass filters and band-stop filters. Low-pass and band-pass harmonic filters are used to filter out the lowest-order harmonics, such as the 5th, 7th, 11th and 13th harmonic orders. Band-pass filters can be single-tuned or double-tuned, meaning they can be configured to filter out one or two harmonic orders. A high-pass filter is used to filter high harmonic orders. The special high-pass filter, the C-type high-pass, is used to provide reactive power and avoid parallel resonance. Figure 2.7 below shows different passive filter topologies used to filter different harmonic orders, and Figure 2.8 demonstrates different filter bands based on each filter topology shown in Figure 2.7 [9].

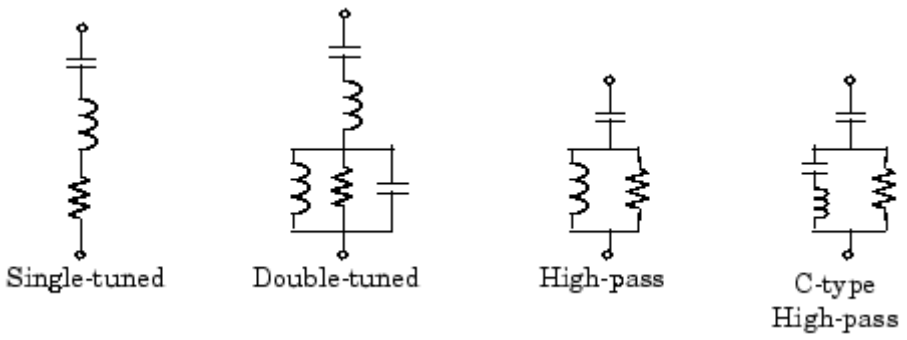

Figure 2.7: Different passive filter topologies used to filter different harmonic orders [7]

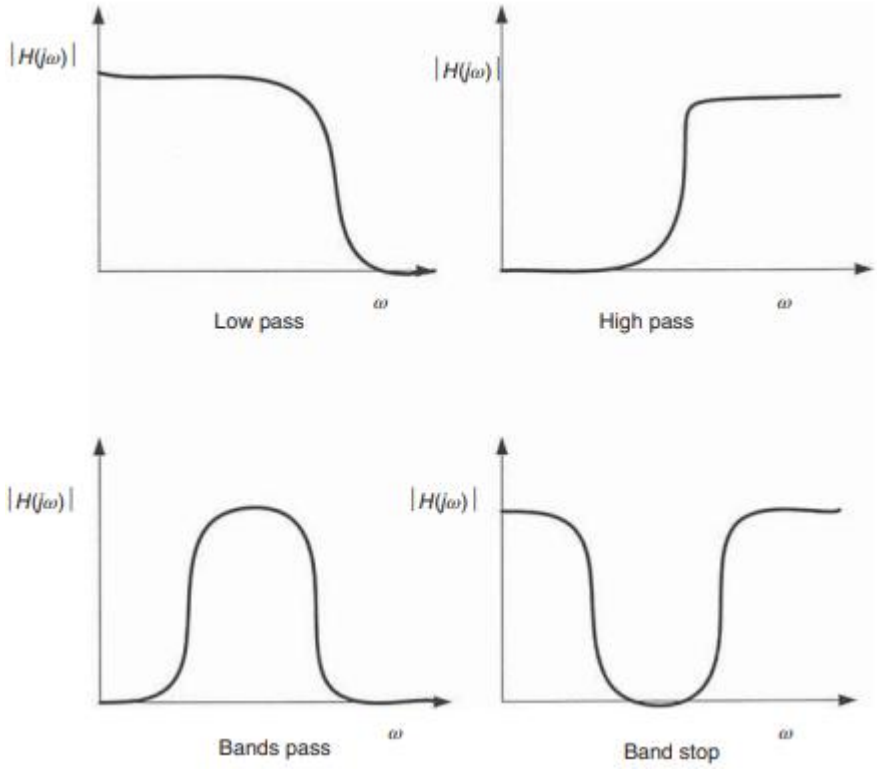

Figure 2.8: Passive filter topologies used to filter different harmonic orders *[9]*

2.6.3. Effects of harmonics

A power network is designed to operate with sinusoidal voltages and currents, when that is not achieved it can negatively affect the grid. The following are some of the effects that comes with harmonics:

I. **Overloaded neutral conductor**: In an ideal balanced three phase network without harmonics, neutral current is said to be zero. This will never be achieved due to harmonics, zero-sequence harmonics results in the neutral conductor and overloads the neutral conductor [23].

II. **Electrical equipment malfunction**: Metering and sensitive instrumentation equipment can take incorrect readings. Close to resonance, higher harmonic voltages may cause sufficient error [9].

III. **Excessive losses, over-voltages, excessive current and heating**: Harmonic currents flowing in the conductors and electrical equipment cause heating effect, which results in overheating of the equipment and insulation derating of the conductors [25]. Distorted voltage causes increased eddy current losses in transformers and motors [23].

2.7. Impact of source impedance on voltage supply waveforms

Source impedance is the impedance of the grid-network; it is dependent on the distance of the customer from the power generation station. It includes all the equipment on the transmission lines, it is the total impedance of the transformers, transmission lines, etc. High impedances involve areas which are relatively far from the power generation station. High impedance can contribute to voltage sags, low voltage conditions, high frequency noise, transient impulses and harmonic voltages [5]. Figure 2.9 below demonstrates equipment that makes up source impedance. In a weak system where the source impedance is high, voltage distortion is high and can cause more problems if harmonic mitigation strategies are not implemented.

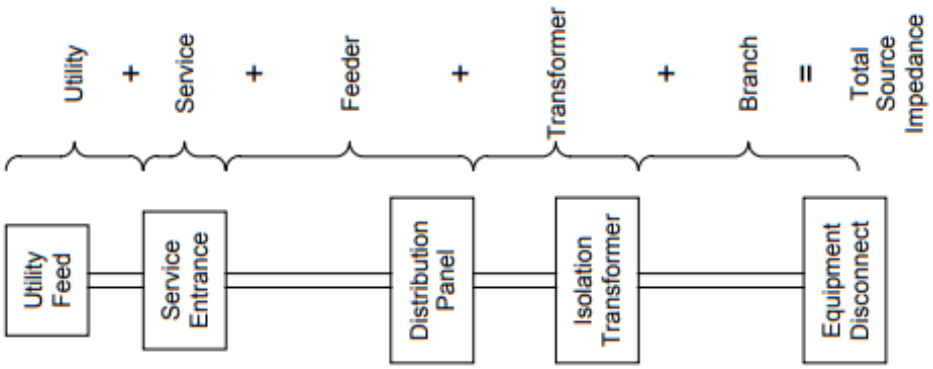

Figure 2.9: Equipment that makes up source impedance *[5]*

2.8. Recent studies on use of passive filters to mitigate harmonics in solar PV systems

Recent studies have been conducted to minimize the harmonics in off-grid and grid-connected solar PV systems. The main aim of these studies, is to study the impact of the passive filter in minimizing the THD. This review will look at the method and simulation tools used for power quality improvement as well the attained results.

2.8.1. Off-grid solar PV system

Adak et al. [7] designed, modelled and simulated a passive LLCL filter for an off-grid solar PV system. The aim is to ensure that both voltage and current waveforms are sinusoidal during energy generation. During modelling, a six-pulse rectifier was used as a non-linear load. The outcome of their simulation results revealed the reduction of total harmonic distortion for current (THDi) from 89.89 % to 3.257 %. However lack of step-by-step analytical filter design equations was identified as gaps not covered by this Adak's study.

Sharma et al. [26] modelled the use of LC passive filter to mitigate the voltage and current related harmonic problems for interleaved solar PV inverter. An LC filter has been connected in series and in parallel to mitigate the voltage related problem and current related problem, respectively. During simulations, P&O and MPPT techniques were applied to track the maximum power point of solar PV panel during changing solar irradiation condition. The results revealed that the total harmonic distortion has been reduced from 24.42% to 4.09% due to the inclusion of a series-shunt LC filter. Hence, dominant harmonics were eliminated from the output voltage to conform with IEEE-519 standards.

Haq, et al. [27] have demonstrated that the use of MPPT algorithms cannot adjust the reference voltage under sudden environmental changes due to cloud, in off-grid solar PV system. This leads to an increasing power loss. To compensate this sudden environmental change, it was

proven that the addition of a modified LCL filter in the system compensate the starting overshoot and sudden undershoot for better stability. Hence, the introduction of the LCL filter enabled both the current overshoot and current sudden cloud undershoot to decrease by 61.648% and 11.915%, respectively. Additionally, both power overshoot and power sudden cloud undershoot proved to decrease by 47.951% and 12.262%, respectively.

Adak and Cangi [28], Modelled and simulated an L and LC passive filter to eliminate the harmonic components of the stand-alone PV power system using of Matlab/Simulink program. LC filter proved to reduce the THDi from 91.55% to 2.62% while the L filter reduced the THDi to 5.73%. Additionally, LC filter also proved to improve the system efficiency.

Aljwary et al. [29] modelled a passive single tuned RLC filter for minimizing the harmonic distortion in a standalone solar PV based micro-grid, using MATLAB/Simulink. The simulations were carried out at different load power factors. The results proved that the single tuned filter successfully mitigated both the total harmonic distortion for voltage (THDv) and total harmonic distortion for current (THDi). THDv has been reduced to values between 68.51% to 100.3% while the THDi has been reduced to values between 49.64% and 53.77%.

Adak [30] modelled and simulated a stand-alone solar PV system with the aim of eliminating harmonic components through the use of an LC passive filter. This proved to be complicated in terms of determining the filter parameters which need to be correctly/precisely calculated. By using the MATLAB/Simulink program, the results of the study proved that the connection of the LC filter reduced the THDi from 91.55% to 2.62%.

Dlamini et al. [31] designed a passive LLCL filter for a standalone PV system for the purpose of reducing the THDi and THDv, through the use of MATLAB/Simulink software. The results proved that the THDv was reduced from 90.88 to 1.967% and THDi was decreased from 74.24% to 1.95%.

2.8.2. Grid-connected solar PV system

Dua and Agrawal [32] investigated the impact of single tuned RLC filter on a grid-connected solar PV system, using ETAP software. The aim of the filter is to mitigate the harmonic and to improve the power factor. The results of the study showed that the THDi level were reduced to 2.78%, 2.46%, and 2.37%, on three separate buses.

Raj et al. [33] provided an analysis of the harmonics mitigation in a grid-connected solar PV system using an LCL passive filter. The filter is designed to reduce the THD of the grid voltage and current as well as the inverter current. The power quality was enhanced by reducing the TDH for the grid voltage, grid current, and inverter current to 0.08 %, 1.17%, and 4.9%, respectively.

Gumilar et al. [34] discussed the optimization of passive shunt filters using detuned reactors and capacitor bank (LC) to minimize the THDv values in a grid-tied solar-PV-wind generator systems in combination with non-linear load. The THDv level were simulated using three different high values of 16.65%, 19.74% and 28.04% as three different simulation scenarios. The detuned reactor and capacitors bank has proved to reduce the three simulated THDv values to low values of 2.61%, 3.04% and 3.36%, respectively.

Muhammad et al. [35] proposed a step by step method for designing an LCL filter parameter with an active damping system for a grid-connected solar PV-Wind-battery based system. An active damp LCL filter was place between the inverter and the utility grid to reduce the inverter switch side harmonics. The results showed a voltage and current THD of 3.82% and 2.14%, respectively.

Xiong et al. [36] performed the harmonic analysis of a grid-connected solar PV generation system connected to a three-bus distribution network under variable solar irradiance, using MATLAB/Simulink program. An adaptive filter was designed using a low-cost series RL

choke circuit and a C-filter in parallel to attenuate the THD of the inverter current and to protect equipment against transient overshoots. The results proved that a low solar irradiance results in an increased THDi of the inverter while it does not affect the total demand distortion of current (THDi) at the point of common coupling. At a low solar irradiance of 200W/m2, the THDi was above the IEEE standard norm before the used of the adaptive filter. Hence, the adaptive filter reduced the THDi from 6.97% to 1.38%.

Shi and Le [37] did a comparative study of different passive filters such as low pass LC, single-tuned, and LC-based T-shaped band-pass filter to mitigate the harmonics of a grid-connected residential solar PV system. These filters proved to successfully reduce the harmonics from 27.7% to 0.71% (low-pass filter), to 6.13% (single-tuned filter), and to 0.15% (band-pass filter).

Hussain and Qureshi [8], did a comparison of different passive filters such as L, LC, LCL, and LLCL filters in a 100 kW three-phase grid-tied solar PV system, through the use of MATLAB/Simulink. The harmonic contents were compared to analyse the best filter. LLCL filter led to a better performance by reducing the THD of the voltage and current to 0.58% and 0.59%, respectively.

Khalil et al. [38] proposed the use of parallel LC passive filters at the output of the inverter in order to reduce the harmonic pollution of a grid-connected PV system, using MATLAB/Simulink program. Parallel passive filter involves the connection of the capacitor in parallel with the inductor. The results showed that the parallel passive filters reduced the current harmonics from 639.97% to 18.77% and the voltage harmonics from 45.60% to 45.57%. The high solar renewable energy penetration of a grid-connected PV systems proved to lead to power quality problems since different solar radiation levels were simulated.

Moyal and Shivam [39] presented a harmonic mitigation model for a grid-connected solar PV system using LCL filter design with a voltage source converter (VSC) control that switches using a pulse width modulation (PWM) technique. The model was developed through the use of MATLAB and the analysis of THD has been done on grid voltage and current. The grid currents have been analysed at different solar irradiance values. The results have proved that the LCL passive filter reduced both the THDv and THDi to 0.06% and 4.77%, respectively. Under lower solar radiation, the THDI was reduced to a higher value of 5.1%.

Zhong et al. [40] presented a new scheme of a passive LLCL filter for the solar PV grid-connected inverter. The new scheme consisting of a new damping structure for the LLCL filter is proposed, using MATLAB/Simulink. The aim is to overcome the shortcoming of the classic LLCL filter since its series damping structure fails to maintain the attenuation at the inverter switching frequency. The results showed that the new proposed LLCL structure is more superior than the classic one in terms of both THDI and resonance.

Al-Sharif et al. [41] evaluated the impact of a grid-connected PV on power quality and voltage profile using large grid-connected 9570 kW PV feeding the hospital in Saudi Arabia, as a case study. A single-tuned filter was used to reduce the THD to the permissible limits. The simulations been carried using ETAP program for the overall project. The results showed a significant reduction in both the individual and overall THD since they were reduced from 10.87%, 17.37%, and 12.11% to 5.81%, 6.52%, and 7.73%, respectively. They proved to be below 8% according to the IEEE standards.

Hosseinpour and Kholousi [42], proposed a method for LCL filter resonance dampening that maintains the stability of the grid-connected solar PV array system as a result of a change in network impedance. The proposed method proved to lead to an improvement in both the efficiency and power quality of the system. The THDi on the grid side was reduced to 1.76%.

The effectiveness of the proposed method was demonstrated through the use of MATLAB/Simulink software.

Ibrahim et al. [43] proposed an optimized shunt LCL using GRG Algorithm for an enhance quality in the operation of a grid-connected PV System. MPPT was investigated based on two alternative approaches such as artificial neural networks (ANN) and cuckoo search (CS). ANN proved to track environmental condition faster than CS system. The generalized reduced gradient (GRG) was used to enhance the power quality issue. The damped LCL filter consisting of a series resistor proved to be the best filter by reducing the THD current from 14.92% to 3% and the THD voltage from 7.3% to 0.029%.

Khalil et al. [44] simulated an LC passive filter to mitigate the THD caused by non-linear load in a 100 kW grid-connected solar PV system, through the use of MATLAB/Simulink program. The results revealed that the THDi of the current delivered to the grid, was reduced from 639.97% to 18.77% in a three-phase inverters while reduced to 15.05% in a single-phase cascaded H-Bridge five level inverter. Hence, the conclusion was drawn that the single-phase cascaded H-bridge five level inverter is the best one for a solar PV system.

Djeghader et al. [45] used single and multiple passive filter technique to mitigate the harmonics in a grid-connected PV system connected to a non-linear load. Due to the presence of a non-linear load, the THD were above the IEEE standard norm. After using the proposed passive filtering technique, the harmonic mitigation results proved to be better when using multiple filters consisting of a combination of the filter tuned at fifth and the filter tuned at seventh harmonic, gave the best results. The THD for the both the grid current and PV current, where reduced to 0.93% and 0.42%, respectively.

Aljarrah et al. [46], modelled a collection of single-tuned passive filters to be used to mitigate the harmonic distortions caused by a combination of a distributed solar PV generators and non-

linear loads connected to the 0.48 kV distribution feeder fed by a 11kV power grid through a 1500 kVA. The results of the study have revealed the usefulness of the proposed passive filter in mitigating the harmonics levels by reducing both the current and voltage THD to 1.64% and 2.13%, respectively; and improving the power factor from 60% to 98%.

2.9. Conclusion

Most of the studies have analysed the harmonics of a solar PV based system through the use of the MATLAB/Simulink software. Under off-grid solar PV energy generation system supplying a non-linear load, both LC and LLCL filters proved to minimize both the THDi and THDv to values far less than the allowable IEEE limits. Hence, these filters are the best options to consider for the off-grid solar PV system, as compared to L filter. Furthermore, LC filters have demonstrated their ability to enhance system efficiency, although determining the appropriate filter parameters can be complex. Studies have shown that using a combination of series and shunt connected LC filters effectively reduces both THDi and THDv in solar PV systems. A study that was carried using RLC filters also resulted in a reduction of harmonics for both voltage and current. However, the measured THD values remained above the IEEE limits.

Under grid-connected solar PV system, the tuned RLC filter proved to minimize both THDi and THDv below the required limits as compared to when used in an off-grid solar PV system. For a grid-connected solar PV system, LCL filters proved to work efficiently by reducing the THD for both grid and inverter current of the system. However, during low solar radiation level, it has proved to minimize the THD of the current to a value above the IEEE limits. In most instances, whenever a pure LC filter is used, it proved to reduce the THD for current and voltage to values greater than the IEEE limits.

None of the above mentioned grid-connected solar PV studies have analysed the harmonics injected by a weak grid-network when designing a filter to mitigate the harmonics.

CHAPTER 3: ANALYSIS OF HARMONICS BASED ON LOAD TYPE AND GRID IMPEDANCE

3.1 Introduction

Before designing a filter that will effectively reduce notable harmonics and clean the distorted AC waveforms, it is essential to comprehensively understand the origins and behaviour of harmonics in power systems. This chapter critically investigates the sources and levels of harmonics as influenced by different load types and grid impedance conditions. Harmonics are currents or voltages at frequencies that are integer multiples of the fundamental frequency (50 Hz in this study) [47]. In this Chapter the behaviour of harmonics is analysed for different configurations using PSIM simulation software with a detailed Fast Fourier Transform (FFT) to extract and quantify order-specific harmonics. FFT is used to separate harmonic orders and present them in a graphical presentation, it extracts fundamental frequency, even and odd harmonic orders and present them with their quantity values in a waveform. This study forms the basis for designing a practical passive filter solution for a weak grid.

3.2 Simulation study

The focus of the simulations conducted is to study the sources of harmonics before implementing the four-branch star passive filter. The simulations will highlight the impact of the load type, grid impedance and solar PV system on current and voltage waveforms. The simulations will also help to understand the effect of source impedance on the grid-connected solar PV system. The line voltage of 400 V will be used during simulations. The current total harmonic distortion is denoted by THDi, and the total voltage harmonic distortion is denoted

by THDv. The PSIM models were developed with explicit assumptions to ensure realistic representation of practical grid conditions:

A. **Time step:** A fixed time step of 1 µs was chosen to capture high-frequency switching effects accurately.

B. **Solver:** The default PSIM simulation solver was used with high-resolution FFT settings to resolve harmonic orders up to at least the 25th.

C. **Component models:** All power electronic components, including inverters, switching MOSFETs, and filters, were modelled with manufacturer-based parameters. The non-linear load includes a bridge rectifier and a smoothing capacitor.

D. **Grid impedance:** Grid strength was varied by adjusting the inductive reactance in the supply lines from 1 mH (strong) to 10 mH (weak). The resistance component was assumed negligible relative to reactance for simplicity, consistent with practical grid impedance modelling.

3.2.1 Linear load on strong grid.

A pure resistive load (100 Ω) was connected directly to a 400 V, 50 Hz AC grid. The simulation confirmed negligible harmonic generation, the supply current and voltage retained near-perfect sinusoidal shapes with THDi and THDv both under 0.1%. No significant higher-order harmonics were observed, as shown in Figure 3.2 and Figure 3.3.

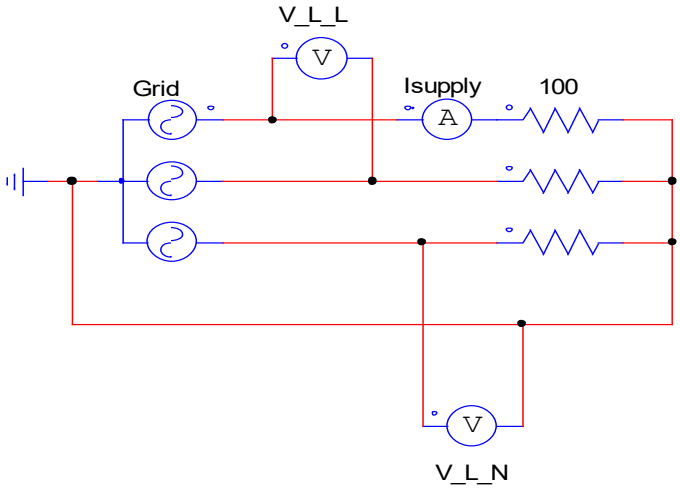

Figure 3.1: Pure resistive load connected directly to AC grid supply

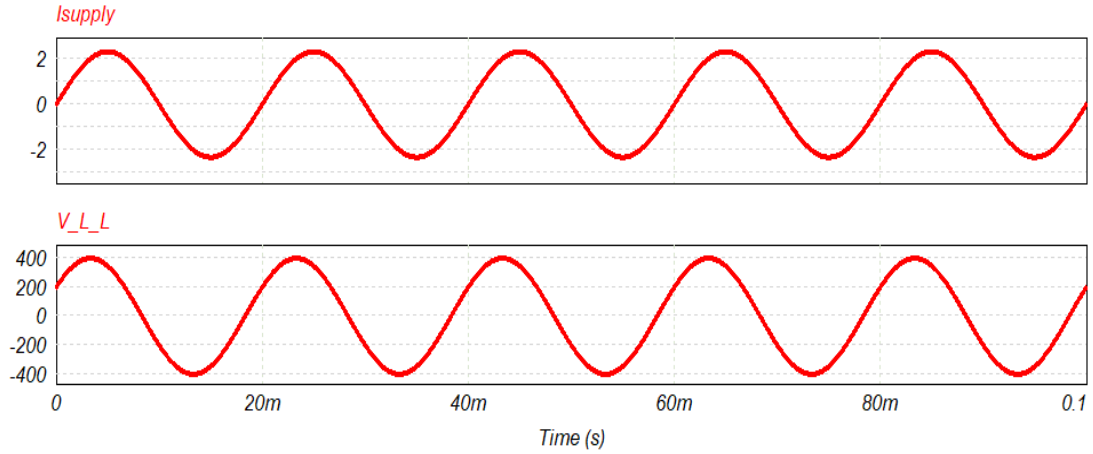

Figure 3.2: Supply current and line voltage simulation results of pure resistive load connected to grid.

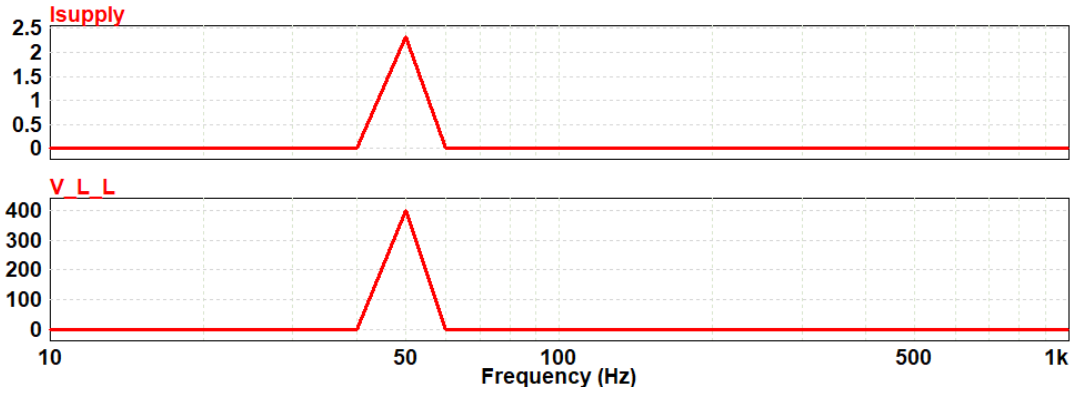

Figure 3.3: Harmonic spectrum of supply current and supply line voltage of linear load connected to grid

3.2.2 Nonlinear load on strong grid.

When a three-phase non-linear load was connected, significant current harmonics appeared due to the power electronic conversion. The FFT showed dominant 3rd (150 Hz), 5th (250 Hz), and 7th (350 Hz) harmonics as shown in figure 3.6. The THDi reached 60.6%, far exceeding the IEEE 519 limit of 5% as shown in figure 3.5. The voltage distortion, however remained within acceptable limits at 0.09% due to the strong grid's low source impedance. A 60 u F capacitor is used to smoothen the ripple on the DC side of the load.

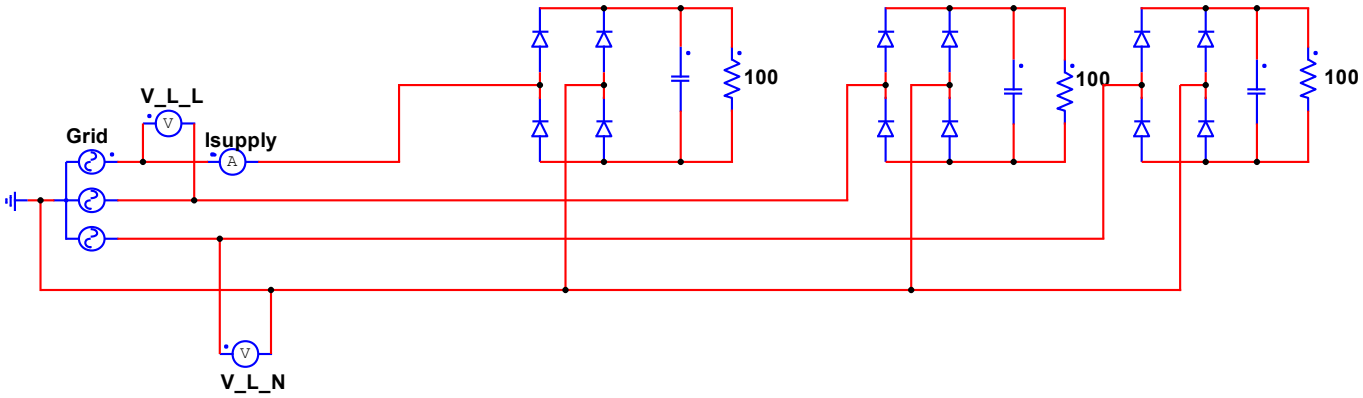

Figure 3.4: Nonlinear load connected to AC grid supply circuit

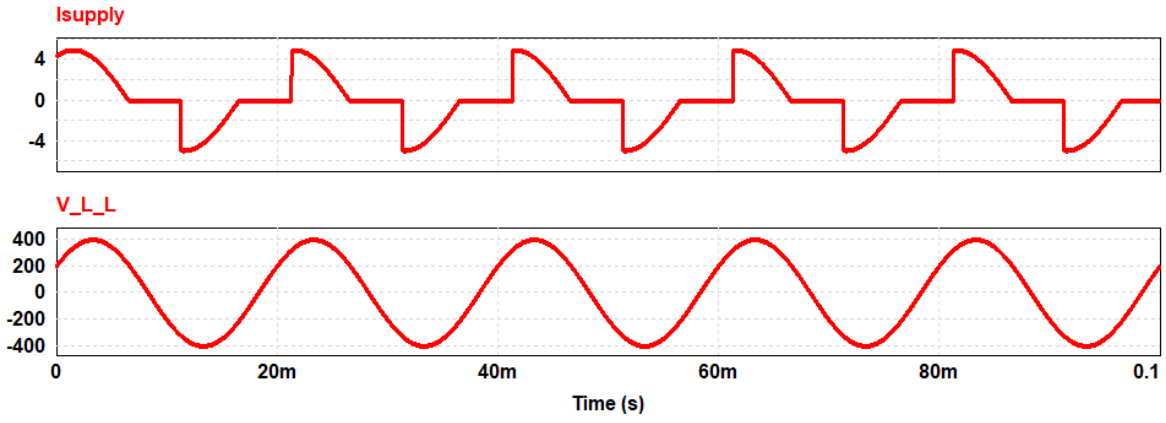

Figure 3.5: Supply current and line voltage waveforms influenced by a nonlinear load connected to grid

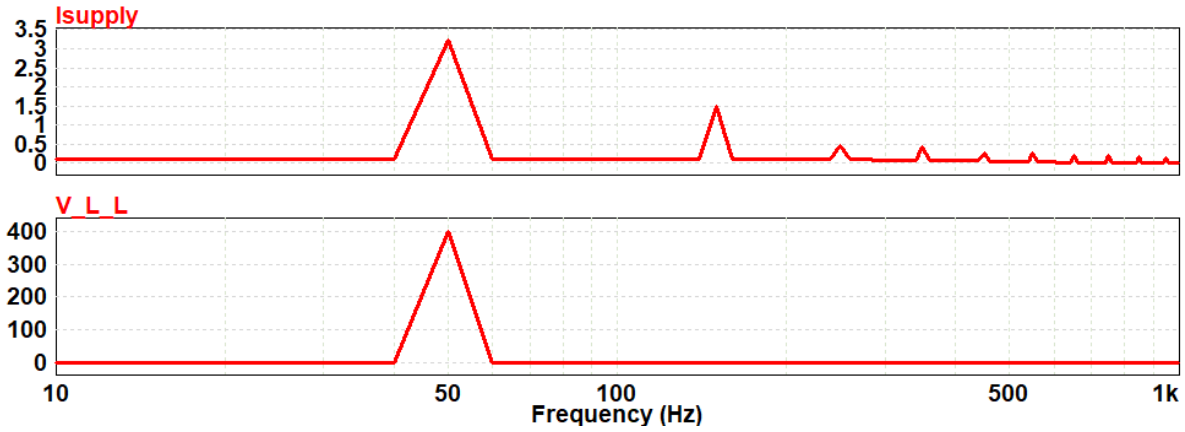

Figure 3.6: Harmonic spectrum of supply current and line voltage as influenced by a nonlinear load

Table 3.1: Total harmonic distortion (p.u) of supply current and line voltage influenced by a non-linear load

	X1	X2	Δ	THD
Time	6.00020e-02	8.00020e-02	2.00000e-02	freq=50
Isupply	1.37680e-08	1.37679e-08	-9.55012e-14	6.05996e-01
V_L_L	2.00216e+02	2.00216e+02	1.43160e-10	9.06739e-04

3.2.3 Weak grid supplying nonlinear load

Due to assumptions made when calculating source impedance value such as all sources are treated as balanced and equal, all 3 phases in power lines have the same impedance, the resistance is negligible; presupposition value of 10 mH has been selected as source impedance in the simulations.

When a utility grid network has lower reactance, it is referred to as a strong grid network; conversely, a network with higher reactance is termed a weak grid network. A grid-network impedance can range from a few mH's and could be overestimated up to 10 mH [48]. In this study, the strength of the grid-network will be changed from a strong up to weak by varying the reactance from 1 mH to 10 mH.

Figure 3.7 shows a non-linear three-phase load supplied by a utility grid having an impedance of 10 mH across each line. When source impedance was increased to 10 mH per phase (representing a weak grid with $Z = j\omega L = j2\pi 50 \times 0.01 = j3.14\,\Omega$), both current and voltage waveforms showed notable distortion. The THDi rose to 89% and THDv to 9.75% as shown in table 3.2, both exceeding IEEE standards. The dominant harmonics are 3rd and 5th harmonics for both voltage and current, as shown in Figure 3.9.

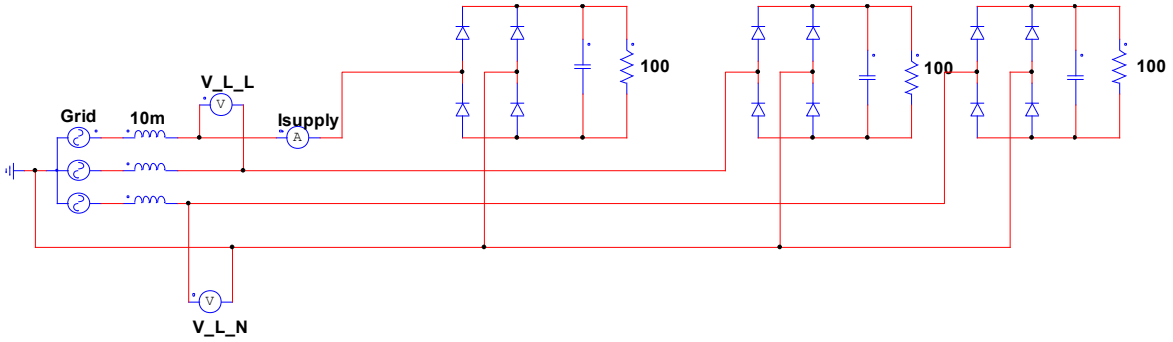

Figure 3.7: A nonlinear load supplied by a weak AC grid-network

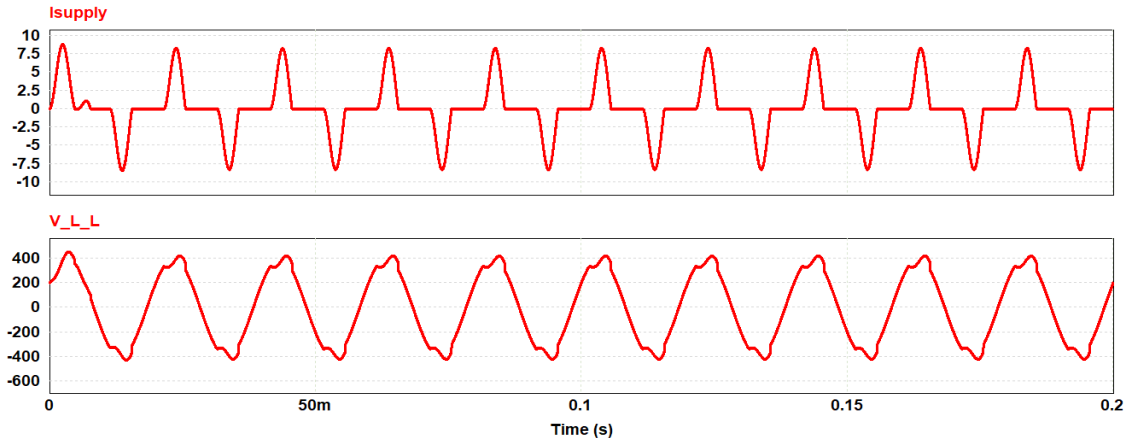

Figure 3.8: Voltage and current waveforms as influenced by a weak grid-network

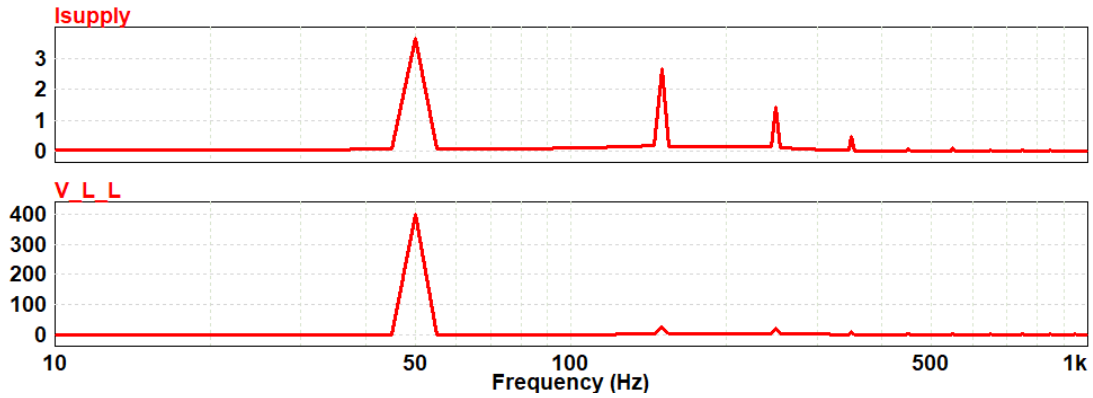

Figure 3.9: Harmonic spectrum of current and voltage waveforms as influenced by a weak grid-network

Table 3.2: Table showing total harmonic distortion (p.u) results of supply current and voltage influenced by a weak grid-network.

	X1	X2	Δ	RMS	THD
Time	1.40002e-01	1.60002e-01	2.00000e-02		freq=50
Isupply	1.36574e-08	1.36575e-08	1.29959e-13	3.42199e+00	8.97953e-01
V_L_L	2.00216e+02	2.00216e+02	2.29818e-10	2.83217e+02	9.74612e-02

3.2.4 Grid-tied Solar PV system with non-linear load

Analysis of harmonics due to the combination of solar PV systems and non-linear loads connected to strong grid network will be simulated and studied in this section. A typical solar PV array with a Vmp of 450 V and an Imp of 7.9 A has been modelled and used, as shown in Figure 3.10. During simulation, it is assumed that the irradiance and temperature are constant at the standard test conditions to generate maximum power output. A three-phase full-bridge switching MOSFET inverter has been used at a switching frequency of 2 kHz to convert DC to AC. A triangular wave voltage source with a 2 kHz frequency and peak voltage of 3 V has been modelled as the reference voltage of the pulse width modulation.

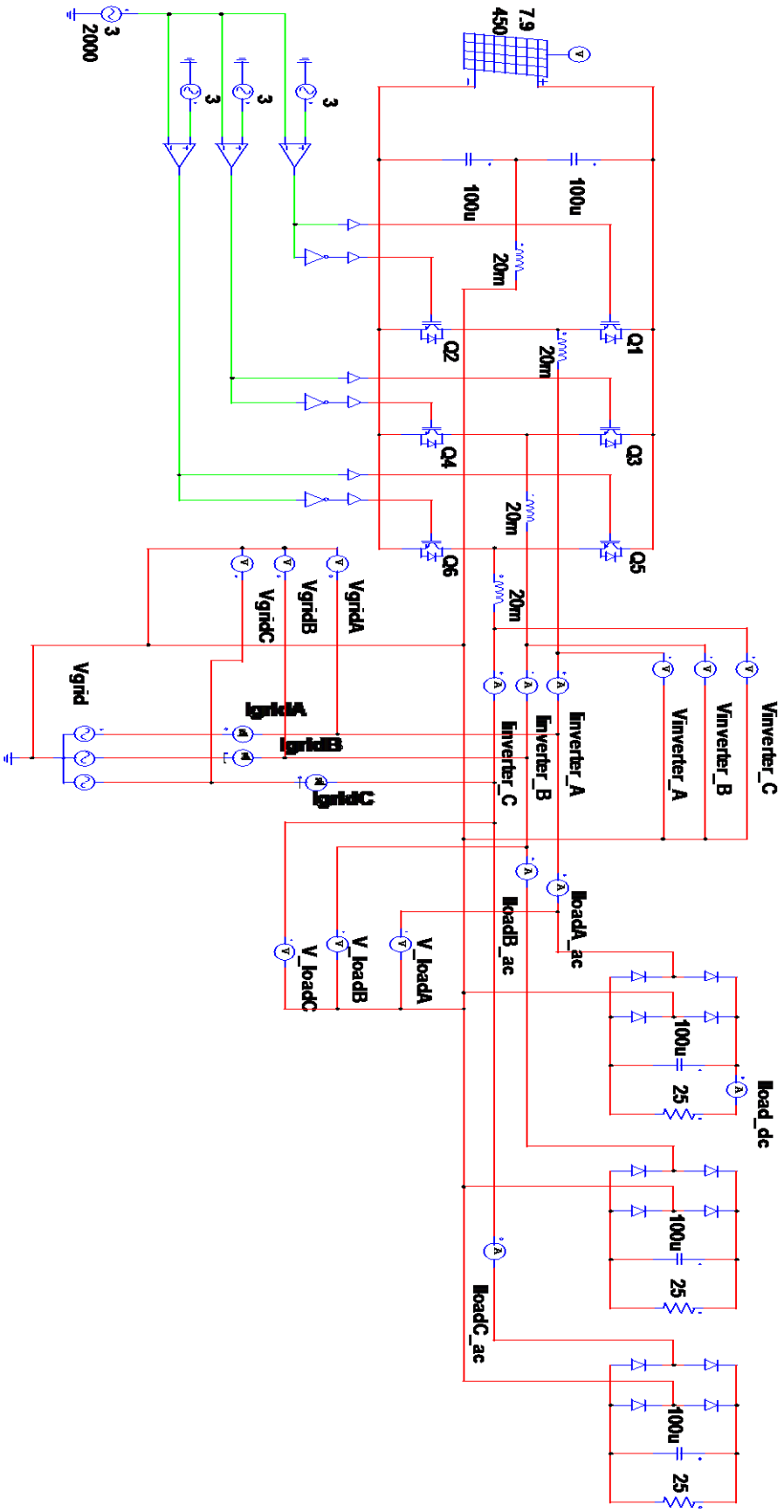

Figure 3.10: Grid-tied solar PV system supplying a nonlinear load

The simulation results of the current and voltage waveforms at the output of the three-phase inverter are as shown in Figure 3.11 to 3.14, as well as in Table 3.3 and 3.4 below. The %THDi of the three-phase current waveform violates the IEEE standard. It ranges between 20.2% and 40.6% with the 2nd, 3rd and 4th order harmonics being the dominants. The output voltage of the inverter proved to be supplying a pure voltage waveform since the %THD is very low at an average value of around 0.087%, as shown in Figure 3.13, 3.14 and Table 3.4.

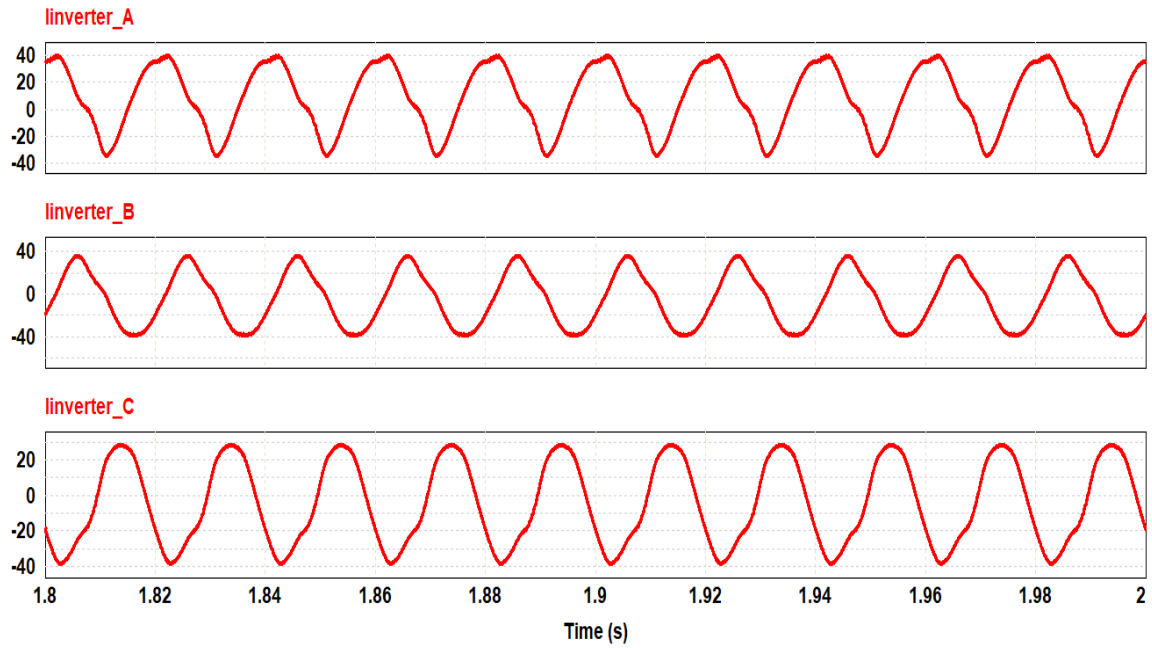

Figure 3.11: Inverter output current

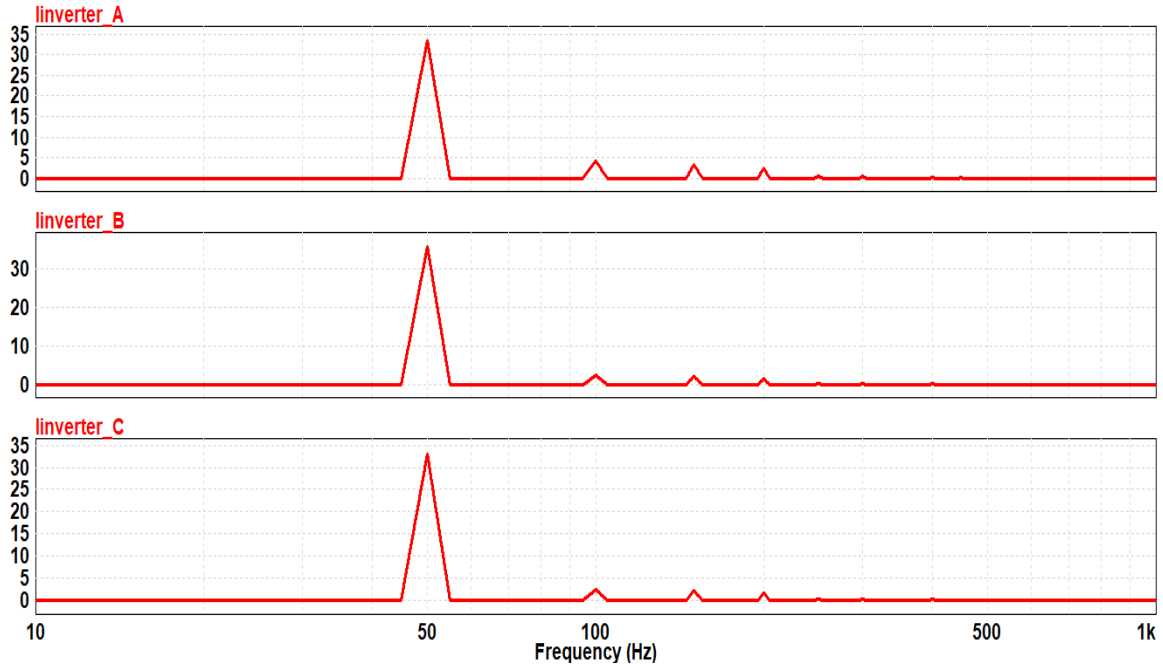

Figure 3.12: Harmonic spectrum of inverter output current waveforms.

Table 3.3: Total harmonic distortion of inverter output current

	X1	X2	Δ	THD
Time	1.83000e+00	1.85000e+00	2.00000e-02	freq=50
Iinverter_A	-2.50636e+01	-2.50625e+01	1.11614e-03	4.05596e-01
Iinverter_B	7.37803e+00	7.37745e+00	-5.77943e-04	2.01917e-01
Iinverter_C	7.67620e+00	7.67878e+00	2.57887e-03	2.07365e-01

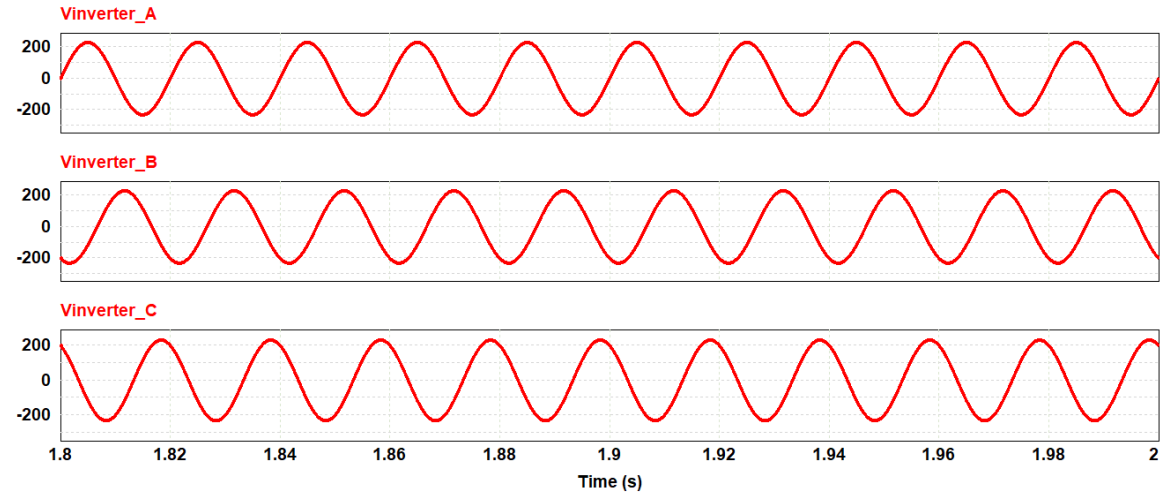

Figure 3.13: Inverter output voltage

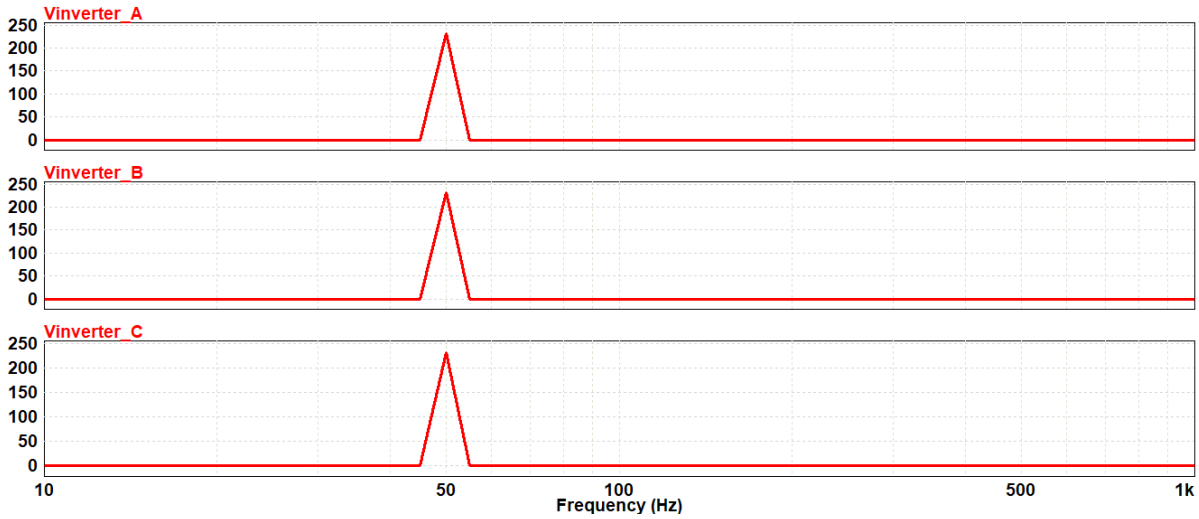

Figure 3.14: Harmonic spectrum of inverter output voltage waveforms.

Table 3.4: Total harmonic distortion of inverter output voltage

	X1	X2	Δ	THD
Time	1.83000e+00	1.85000e+00	2.00000e-02	freq=50
Vinverter_A	-5.10311e-05	-5.12939e-05	-2.62842e-07	9.41104e-04
Vinverter_B	1.99999e+02	1.99999e+02	1.31883e-07	8.34933e-04
Vinverter_C	-1.99999e+02	-1.99999e+02	1.37193e-07	8.34990e-04

The simulation results of the current and voltage supplied to the non-linear load by the combination of a strong grid-network and the inverter, are as shown in Figure 3.15 to 3.14 as well as Table 3.5 and 3.6 below. The %THD of the three-phase load current waveforms violates the IEEE standard limit. They range around 29.6% with the odd harmonics (3rd, 5th, 7th) being the dominants. The voltage across the non-linear load proved not to violate the IEEE standard limit since the grid-network is strong.

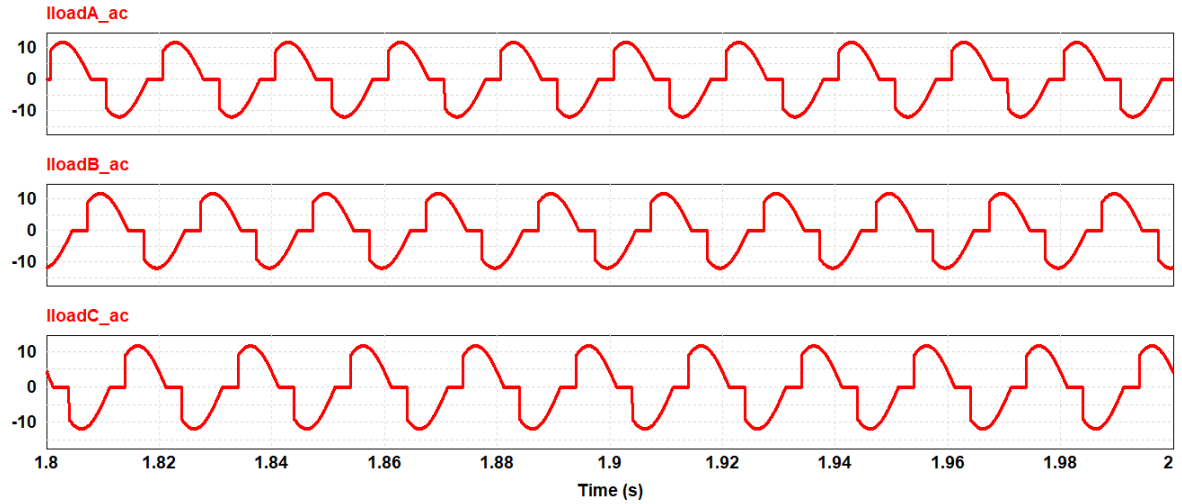

Figure 3.15: Non-linear load current waveforms for the Grid-tied PV system (strong grid)

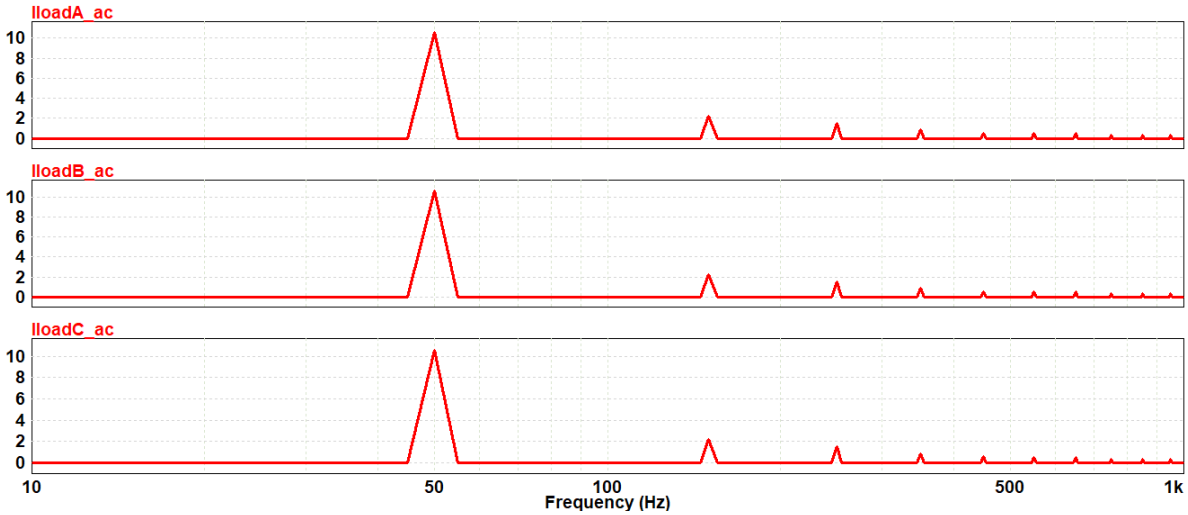

Figure 3.16: Harmonic spectrum of non-linear load current waveforms

Table 3.5: Total harmonic distortion of load current

	X1	X2	Δ	THD
Time	1.83000e+00	1.85000e+00	2.00000e-02	freq=50
IloadA_ac	2.77558e-09	2.77556e-09	-2.55668e-14	2.97385e-01
IloadB_ac	1.16325e+01	1.16325e+01	-1.40631e-07	2.95892e-01
IloadC_ac	-4.37735e+00	-4.37735e+00	3.69435e-08	2.96645e-01

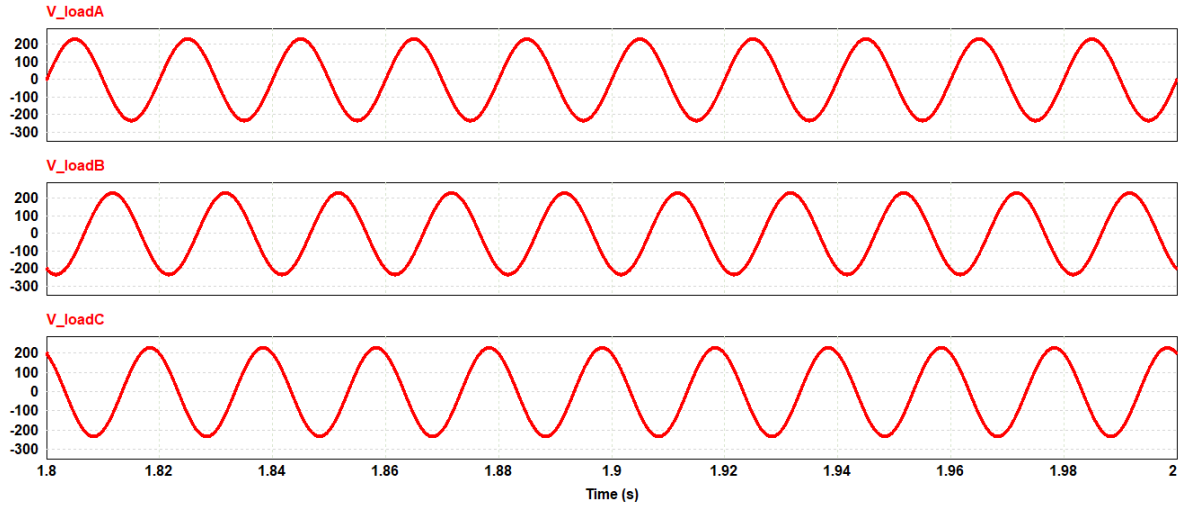

Figure 3.17: Non-linear load voltage waveforms for the Grid-tied PV system (strong grid)

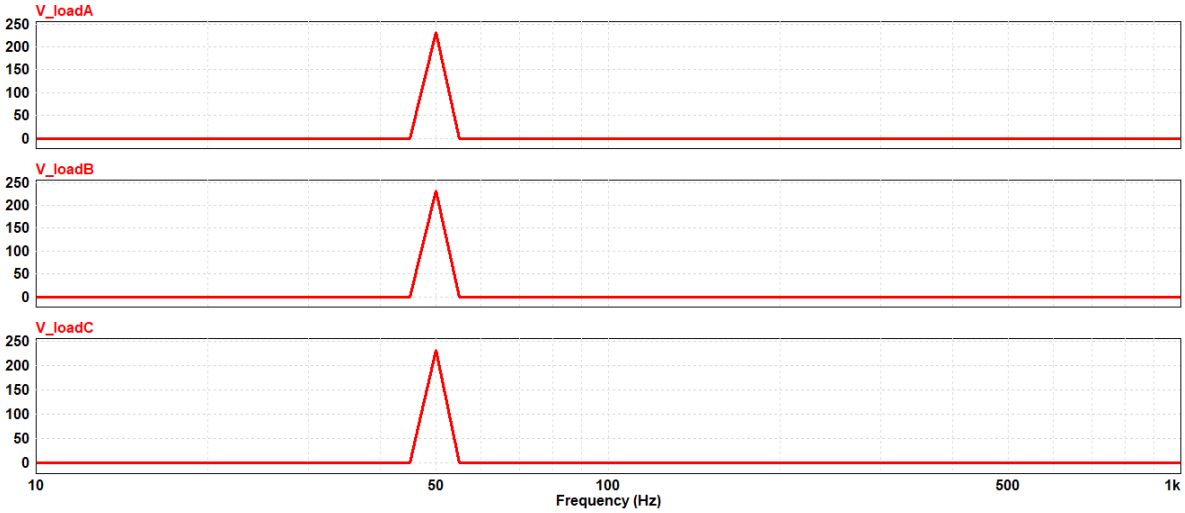

Figure 3.18: Harmonic spectrum of non-linear load voltage waveforms

Table 3.6: Total harmonic distortion of non-linear load voltage

	X1	X2	Δ	THD
Time	1.83000e+00	1.85000e+00	2.00000e-02	freq=50
V_loadA	-2.59674e-05	-2.62314e-05	-2.63958e-07	9.41126e-04
V_loadB	1.99999e+02	1.99999e+02	1.32461e-07	8.34953e-04
V_loadC	-1.99999e+02	-1.99999e+02	1.34615e-07	8.34978e-04

The combination of both the solar PV system and non-linear load proved to negatively affect the supply current from the grid, as shown in Figure 3.19. The harmonics generated by this combination is injected to the utility grid-network and distort grid AC current waveforms. This has led to a %THDi ranges between 23.7 to 51% with the combination of both odd and even harmonics being the dominants, as shown in Figure 3.20 and Table 3.7.

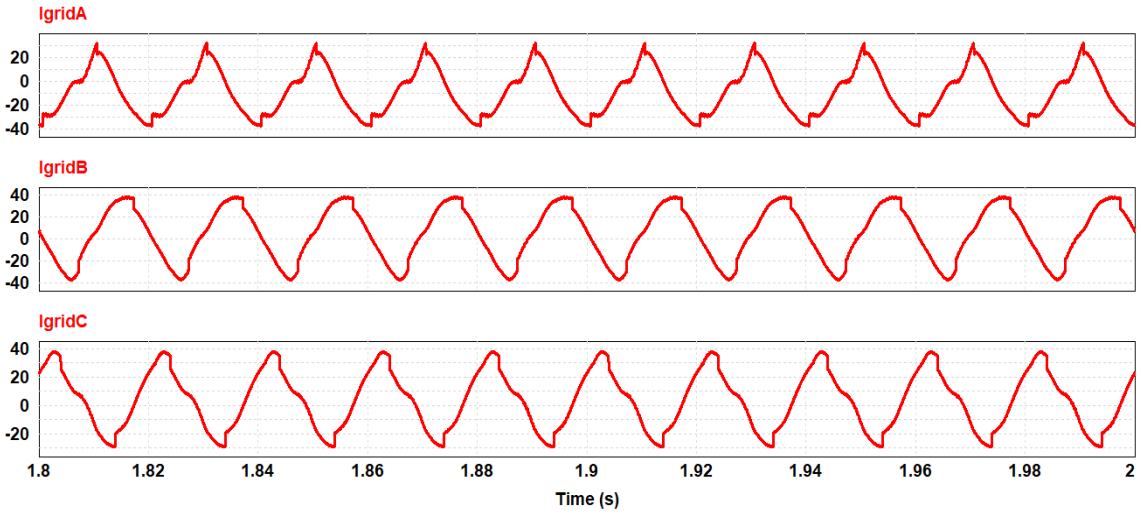

Figure 3.19: Grid current waveforms for Grid-tied PV system with nonlinear load drawing current

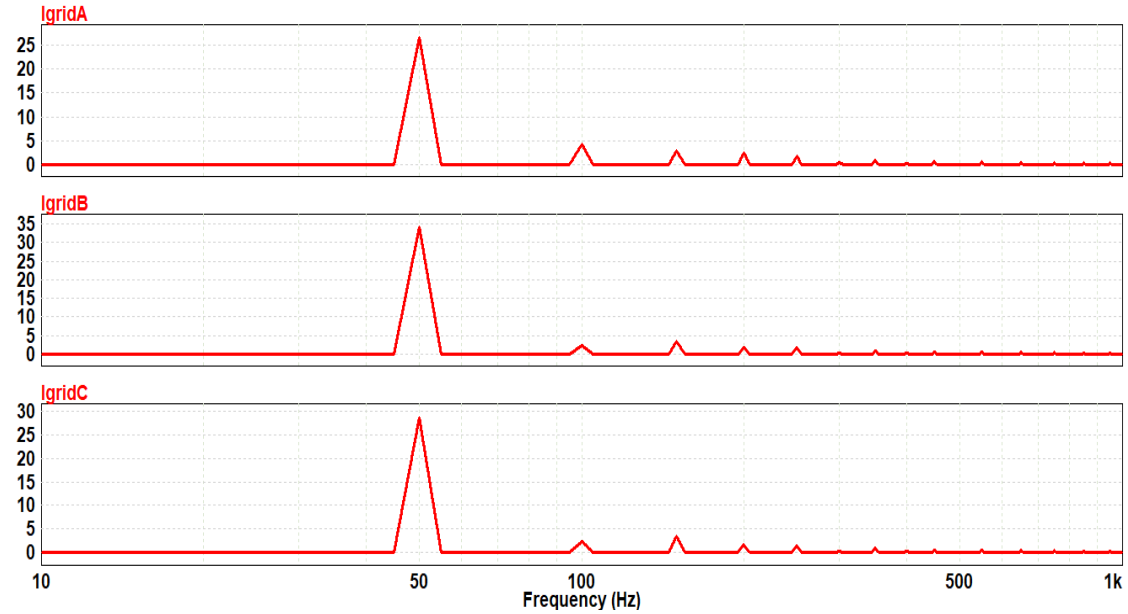

Figure 3.20: Harmonic spectrum of load current waveforms for Grid-tied PV system with nonlinear load drawing current

Table 3.7: Total harmonic distortion of grid current

	X1	X2	Δ	THD
Time	1.83000e+00	1.85000e+00	2.00000e-02	freq=50
IgridA	2.50636e+01	2.50625e+01	-1.11614e-03	5.13708e-01
IgridB	4.25445e+00	4.25502e+00	5.78115e-04	2.37289e-01
IgridC	-1.20535e+01	-1.20561e+01	-2.57889e-03	2.67552e-01

3.3 Comparative Summary

Table 3.1 to Table 3.7 present the individual results for each configuration. For clarity, Table 3.8 below summarises the key THDi and THDv results across all scenarios:

Table 3. 8 Comparative summary of the results

Scenario	**Grid Impedance**	**THDi (%)**	**THDv (%)**	**Dominant Orders**
Linear Load (Strong Grid)	1 mH	0.0	0.0	None
Non-Linear Load (Strong Grid)	1 mH	60.6	0.09	3rd, 5th, 7th
Non-Linear Load (Weak Grid)	10 mH	89	9.75	3rd, 5th
Grid-Tied PV Inverter Output	1 mH	20.2–40.6	0.087	2nd, 3rd, 4th
PV + Non-Linear Load (Strong Grid)	1 mH	29.6	0.1	3rd, 5th, 7th
Grid Supply Current (PV + Load)	1 mH	23.7–51	0.1	Even + Odd

3.4 Conclusion

This chapter has presented a detailed PSIM simulation study describing the sources of harmonics, critically analysing harmonic orders beyond just THD, and highlighting the impact of grid impedance. A weak grid, defined by a source reactance of up to 10 mH ($Z = j3.14\ \Omega$), was shown to amplify both current and voltage distortions, worsening power quality significantly. These insights justify the design and tuning of a passive filter in subsequent chapters, with targeted mitigation of dominant harmonics identified on this chapter.

CHAPTER 4: DESIGN OF FOUR BRANCH RCL HARMONIC PASSIVE FILTER

4.1. Introduction

In this chapter a four-branch RLC filter has been proposed to minimise the harmonics from a weak grid network, solar PV system, and non-linear load. The RLC passive filter consists of a resistor, capacitor, and inductor in each branch of the three-phase, four-wire network. The filter is designed in a configuration that enables it to filter out multiple harmonics from different sources. The filter resonates at a specific frequency that needs to be filtered, which leads to low impedance to those frequencies being eliminated and high impedance to fundamental frequency on the system. The PSIM software tool will be used when designing and tuning the filter to analyse the filter's functionality and its effectiveness. The effectiveness of the filter will be studied in two different cases. The first case is whereby the solar PV system supplying a non-linear load is connected to the strong grid network, and the second case is whereby the solar PV system is connected to the weak grid network. The proposed filter is expected to minimise the THDi and THDv to within the allowable IEEE standard limit for both cases.

4.2. Circuit diagram of the PV grid-tied system with RCL filter

Figure 4.1 shows the simplified single-line circuit diagram of the PV grid-tied system with a RLC filter connected to the grid network. The designed four-branch star RLC passive filter topology consists of identical three-phase branches. Each phase consists of a resistor, a capacitor, and an inductor. The fourth phase connected to neutral has its own unique impedance consisting of a damping resistor and an inductor. The impedances of the three identical branches will be denoted by Z_f, and the impedance of the fourth branch connected to neutral will be denoted by Z_n.

The topology of the designed passive filter will consider positive-, negative- and zero-phase sequence harmonic components. Each component with its impedance will be calculated separately using different formulas. The four-filter branches are resonance cells. The neutral branch will be tuned to filter zero harmonic components, and the other three branches will be tuned to filter out positive-negative-dominant harmonic components. PSIM software will assist with the analysis to show the impact brought by the filter on harmonic. The THD and FFT functions will be used to analyse harmonic content on the network.

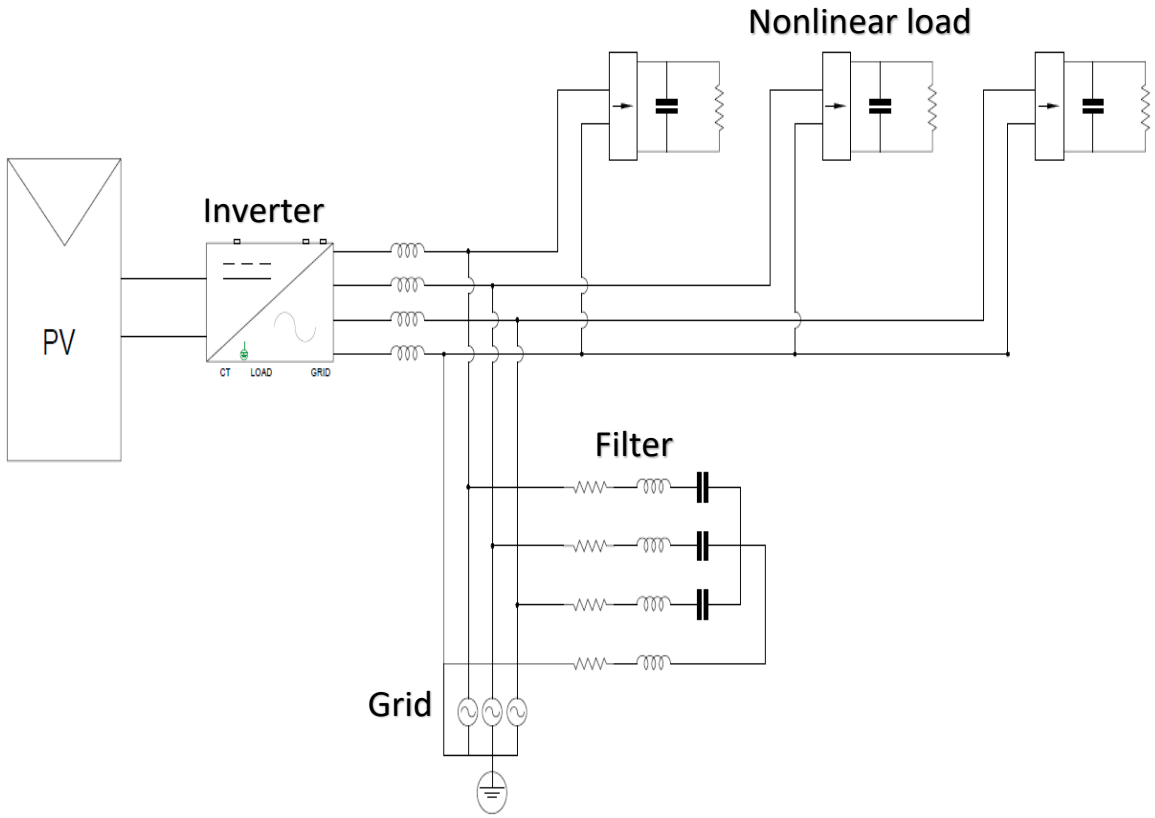

Figure 4.1: Single line circuit diagram of PV grid-tied system with RCL filter

The filter is located near to the sources of harmonic generators so that harmonics can be trapped at the source and limited to the point of common coupling (PPC) to protect the grid, this reduces harmonic emission to the source. On the designed filter, the three branches will filter out non-zero harmonic orders while neutral branch will be tuned to filter out zero harmonic orders and this will be done by selecting appropriate resonant cells of the passive components (inductor,

capacitor, and resistor) on the filter. The impedance of the harmonic filter that will be designed is frequency dependent and will be tuned to provide low impedance for dominant harmonic orders to be filtered in the load current. The filter capacitance (C_f), filter resistance (R_f), resonance frequency (f_o), positive-negative resonant frequency (f_{12}) and damping resistor (R_n) are determined before tuning the filter. The inductors (L_c) between the inverter and the grid/load are the coupling inductor which serve as a filter inductor to smoothen out and filter out unwanted DC ripples.

4.2.1. Design of a positive-negative sequence single-tuned RCL filter

This section covers step-by-step filter design process to be followed.

A. Filter topology and purpose of each branch

The branch is connected in shunt of each live line of the three phases of the grid. Each branch having low impedance for the harmonic order to be filtered. Figure 4.2 below shows RCL branch circuit to be connected to each phase of the network.

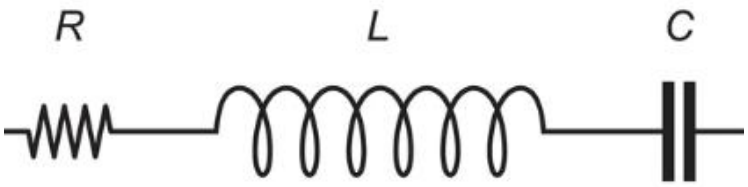

Figure 4. 2: RCL passive filter branch

Appropriate values of the resistor, inductor and capacitor will be calculated in order to eliminate targeted harmonics at resonance.

B. Selection of tuning frequencies

The first step in determining the filter parameters is to know and determine positive-negative resonance frequency (f_{12}), followed by zero resonance frequency. The f_{12} depends on the filter capacitance (C_f) and filter inductance (L_f) and will be determined as follows [22]:

$$f_{12} = \frac{1}{2\pi\sqrt{L_f\, C_f}} \tag{4.1}$$

From the simulation, it was noted that the dominant positive-negative harmonic order is the 5th harmonic order which is 250 Hz. Therefore the f_{12} tuning frequency is determined to be 250 Hz.

C. Step-by-step design equations

I. Filter Capacitance (Cf)

C_f is determined using Equation 2 and the reactive power of the filter ($Qcmax$) is estimated at 5% of the rated output power of the inverter [49]. The rated power of the inverter simulated in this study is 25 kW inverter. 25 kW inverter was selected due to the limitation of the student version of PSIM software.

$$C_f = \frac{Qcmax}{2\pi f v^2} \tag{4.2}$$

$$C_f = \frac{5\%Prated}{2\pi f v^2} \tag{4.3}$$

$$= \frac{0.05\times25000}{2\pi\times50\times230^2}$$

$$= 75.2\ \mu F$$

II. Filter Inductance (Lf)

From the positive-negative resonant frequency (f_{12}) shown in Equation 1, filter inductance (L_f) can be determine for each of the 3 identical branches of the RCL filter as shown by Equation 4.

$$L_f = \frac{1}{4\pi^2(f12)^2 C_f} \tag{4.4}$$

$$L_f = 5.39\ \text{mH}$$

The calculated values of C_f and L_f are the values that will be used in the filter to eliminate dominant harmonic (3rd and 5th) at resonance.

III. Damping resistor (Rf)

The filter consists of a damping resistor that is denoted by R_f on each branch. The damping resistor is selected precisely by ensuring the positive-negative quality factor (Q_{12}) is within the recommended parameter which is between 10-50 [50]. The positive-negative quality factor is determined as follows [51]:

$$Q_{12} = \frac{1}{R_f} \times \sqrt{\frac{L_f}{C_f}} \tag{4.5}$$

Since Q_{12} is selected to be 40, the damping resistor of positive-negative branch is therefore determined as follows:

$$R_f = \frac{1}{Q_{12}} \times \sqrt{\frac{L_f}{C_f}} \tag{4.6}$$

$$R_f = 0.212\Omega$$

IV. Weak grid positive-negative sequence shifted tuning frequency (f_{12n})

When the source impedance is considered on the system, there will be a new resonant frequency for positive-negative harmonic components. The frequency will be shifted by the source impedance inductance (L_s). Equation 7 below is used to determine the new positive-negative resonant frequency that includes source impedance and is denoted by f_{12n} [51].

$$f_{12n} = \frac{1}{2\pi\sqrt{(L_s+L_f)\times C_f}} \tag{4.7}$$

The reason for determining f_{12n} is to ensure that the filter is effective whenever the source impedance is taken into consideration in the system. It is expected that resonance condition

with the source impedance may worsen the harmonic distortion of the supply by amplifying the load harmonic components of the system [22]. When Ls=10 mH, the new shifted frequency (f_{12n}) is 244,8 Hz.

4.2.2. Design of a zero-sequence neutral branch of a RCL filter

A. Selection of tuning frequencies (f_0)

The dominant zero-sequence harmonic order (f_0) to be eliminated is the 3rd harmonic component (150 Hz).

B. Selection of filter inductor (Ln)

The neutral branch inductance (L_n) of the filter is determined using equation 8 [51].

$$L_n = \frac{1}{12\pi^2 {f_0}^2 C_f} - \frac{1}{3} L_f \tag{4.8}$$

$$L_n = 3.19\ mH$$

C. Selection of a damping resistor (R_n)

The damping resistor on the neutral branch (R_n) of the filter is determined from the zero-sequence quality factor (Q_0). The quality factor is also selected between 30–40 for good tuning of the filter. The selected quality factor that proved to produce good results is 39. The trial method was used to select the R_n value that would give a result of Q_0=39 as the selected zero-sequence quality factor. Using Equation 9, R_n value of 0.05 Ω has been determined and used since it led to the required Q_0. This was achieved using Equation 9 [51].

$$Q_0 = \frac{1}{R_f + 3R_n} \times \sqrt{\frac{L_f + 3L_n}{C_f}} \tag{4.9}$$

D. Weak grid zero sequence shifted tuning frequency (f_{on})

The source impedance shifts the zero harmonic component resonance. New frequency resonance is given by Equation 10 whenever the resonance is affected by source impedance [51].

$$f_{0n} = \frac{1}{2\pi\sqrt{(L_s+L_f+3L_n)\times C_f}} \tag{4.10}$$

When Ls = 10 mH, the new shifted frequency (f_{0n}) is 148,7 Hz. This value confirms tuning drift under weak grid conditions and ensures that the drift has been compensated on the design.

4.2.3. Frequency domain plot of filter impedance

A frequency range from 10 Hz to 1000 Hz was selected to capture the harmonic spectrum that includes the dominant harmonics to prove the resonance of the filter. The calculated filter component values (Cf = 75,2 uF; Lf = 5.39 mH; Rf = 0.212 Ω) were used to calculate the impedance of each component, as shown below:

- Capacitive impedance: Zc = 1 / (jωCf)
- Inductive impedance: Zl = jωLf
- Resistor: Zr = Rf
- Impedance magnitude: Z_total = Zr + Zl + Zc

The table below shows values used to plot the frequency domain plot of the RCL filter in step intervals of 50.

Table 4. 1 Impedance vs frequency RCL filter data

Frequency (Hz)	Impedance Magnitude (Ohms)
10	211,3036542
10,99099099	192,187609
50,63063063	40,08710469
100,1801802	17,73468425
250,8108108	0,219202844
300,3603604	3,133019212
350,9009009	5,856182392
400,4504505	8,279413695
450	10,53883822
500,5405405	12,72498352
550,0900901	14,783664
600,6306306	16,81884799
650,1801802	18,76530764
700,7207207	20,71160097
750,2702703	22,5890449
800,8108108	24,47862322
850,3603604	26,31061849
900,9009009	28,16181159
950,4504505	29,96229859
1000	31,75065446

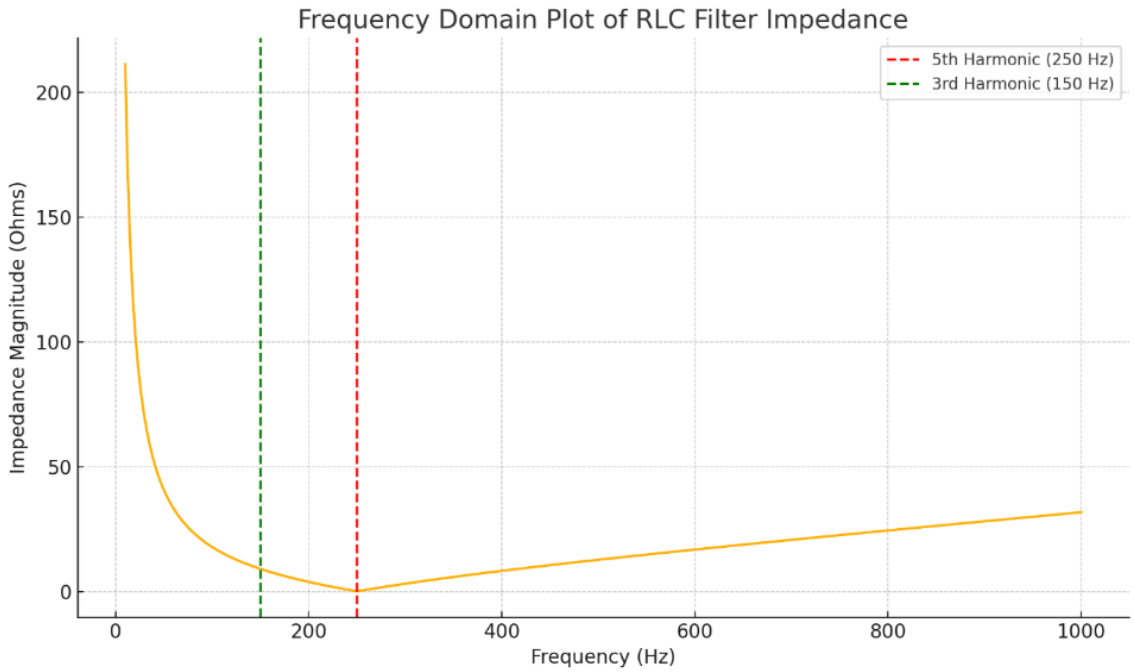

Figure 4. 3 Frequency domain plot of RCL filter impedance

4.3. Simulation circuit

A grid-tied solar PV system with nonlinear load connected was simulated. The inverter has been modelled to ensure it meets the grid code by syncing with the grid. For a good inverter model, there are conditions that need to be met such as frequency, voltage and phase angle. All the conditions needs to sync with the grid. Table 4.1 shows the parameters used to simulate the system as well as the design parameters of the proposed RLC filter. The overall circuit diagram of the simulated grid-tied solar PV system with nonlinear load and the designed RLC filter is as shown in Figure 4.3 below. The filter will be employed to eliminate the dominant harmonics in two scenarios: when the solar PV system is connected to a strong grid network and when it is connected to a weak grid network.

Table 4.2: Simulated circuit parameters

Circuit parameters	**Values**	**Unit**
Source Impedance **(Ls)**	10	mH
Load Capacitor	400	µF
Load Inductor	1	mH
Load Resistor	5	Ω
Phase voltage **(Vrms)**	230	V
Line Voltage **(Vl)**	400	V
System frequency	50	Hz
Filter Capacitor **(Cf)**	75,2	µF
Filter Inductance **(Lf)**	5,39	mH
Filter resistor **(Rf)**	0.212	Ω
Neutral branch Inductance **(Ln)**	3,19	mH
Neutral branch Resistor **(Rn)**	0.05	Ω
Fifth harmonic **(f12)**	250	Hz
Zero harmonic **(f0)**	150	Hz
Shifted **(f12n)**	244,8	Hz
Shifted **(f0n)**	148,7	Hz
Positive-negative component Quality factor **(Q12)**	40	Unit
Zero component Quality factor **(Q0)**	39	Unit
Solar Open Circuit Voltage **(Voc)**	1000	V
Solar Short Circuit Current **(Isc)**	40	A
Solar Maximum Power Voltage **(Vm)**	980	V
Solar Maximum Power Current **(Im)**	36	A
Inverter series inductor	20	mH
Solar neutral split capacitors	500	µF

4.4. Simulation Results

4.4.1. Synchronisation of the inverter with the grid

To synchronise the grid with the inverter, a hysteresis current controller is modelled. The inverter is modelled to be a current controlled inverter. The hysteresis controller continuously compares the sensed filtered inverter output current with the reference set value of the hysteresis controller to adjust the gate signals to the inverter switches and ensuring that the inverter output current is within the hysteresis band limit, as shown in Figure 4.4 below. Hysteresis band limit is the band formed by two signals to ensure the inverter output current is within the range of the set value. One signal is lower than the reference value and the other signal is higher than the reference, both by 0.25 A. The algorithm that the hysteresis controller uses is that when the inverter output current is greater than the upper band, the current is allowed to decrease by turning OFF the top switch and turning ON the bottom switch of the inverter leg.

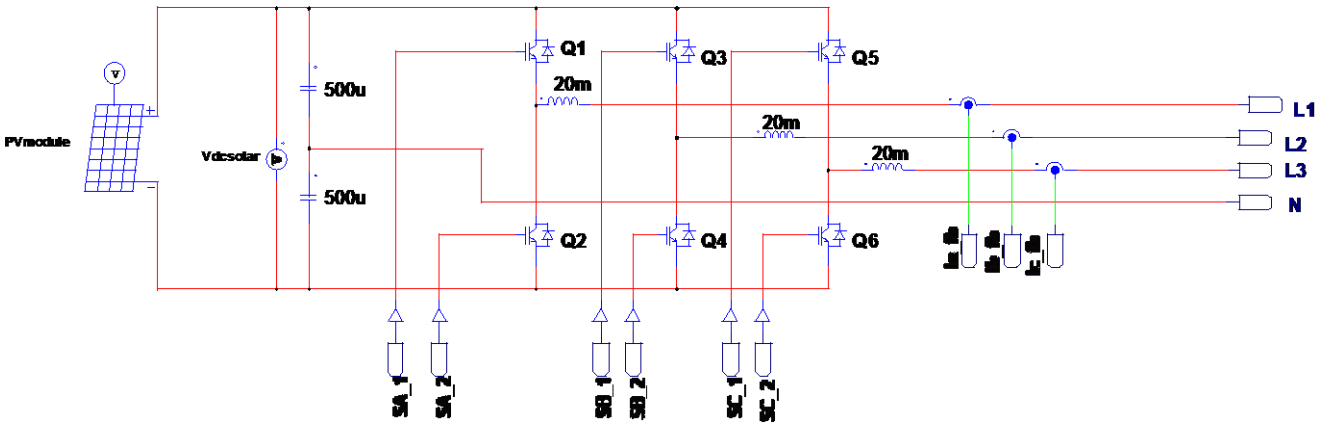

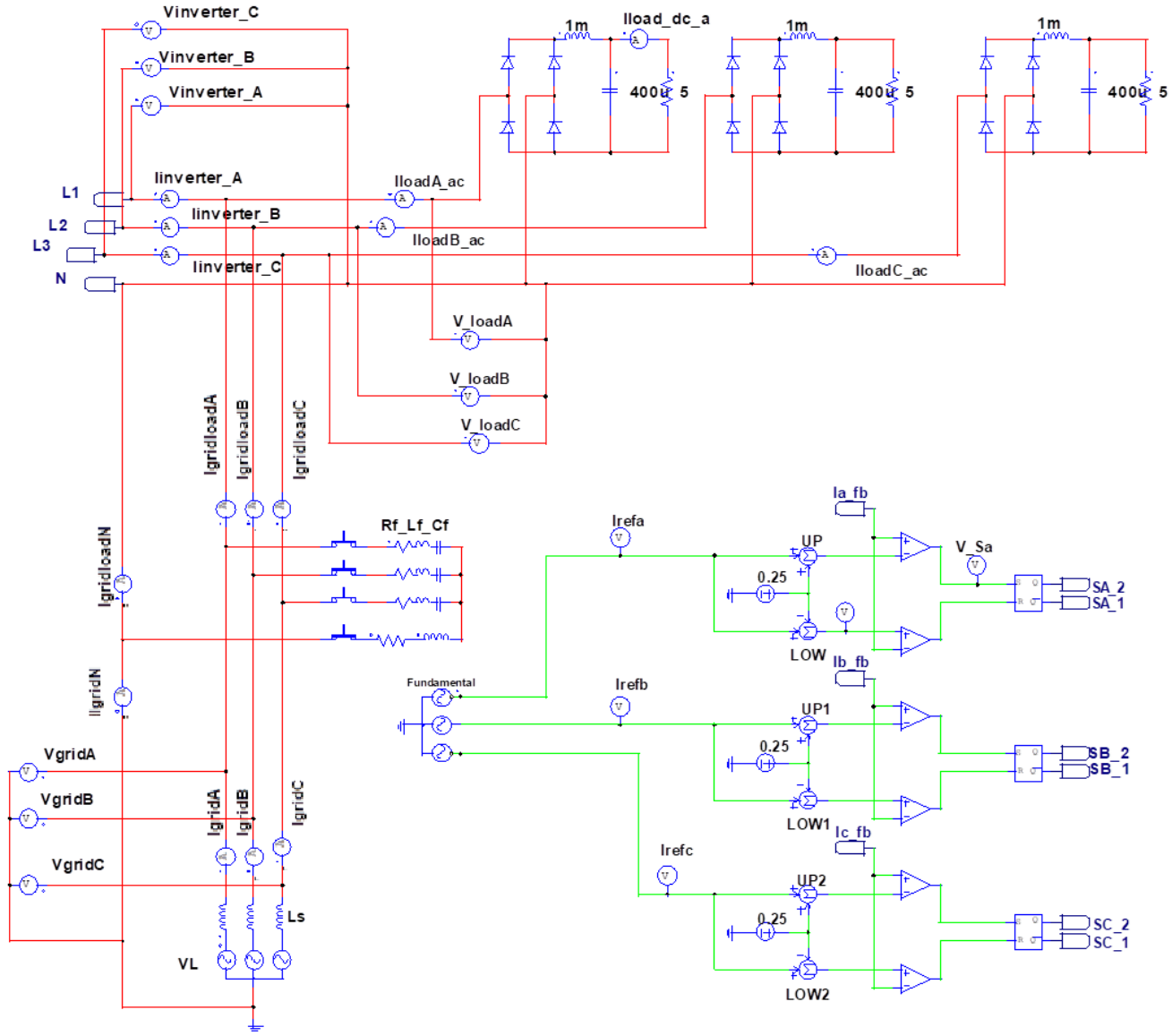

Figure 4.4: Grid-tied solar PV simulated circuit diagram with nonlinear load and RLC filter

When the inverter output current goes below the lower band, the current is allowed to increase by turning ON the top switch and turning OFF the bottom switch. Within the band limits of the hysteresis current controller, the state of the controller is latched until the filter current exceeds the next band. Below are the results of the hysteresis band set to 0.5 A (i.e ± 0.25 A the reference current).

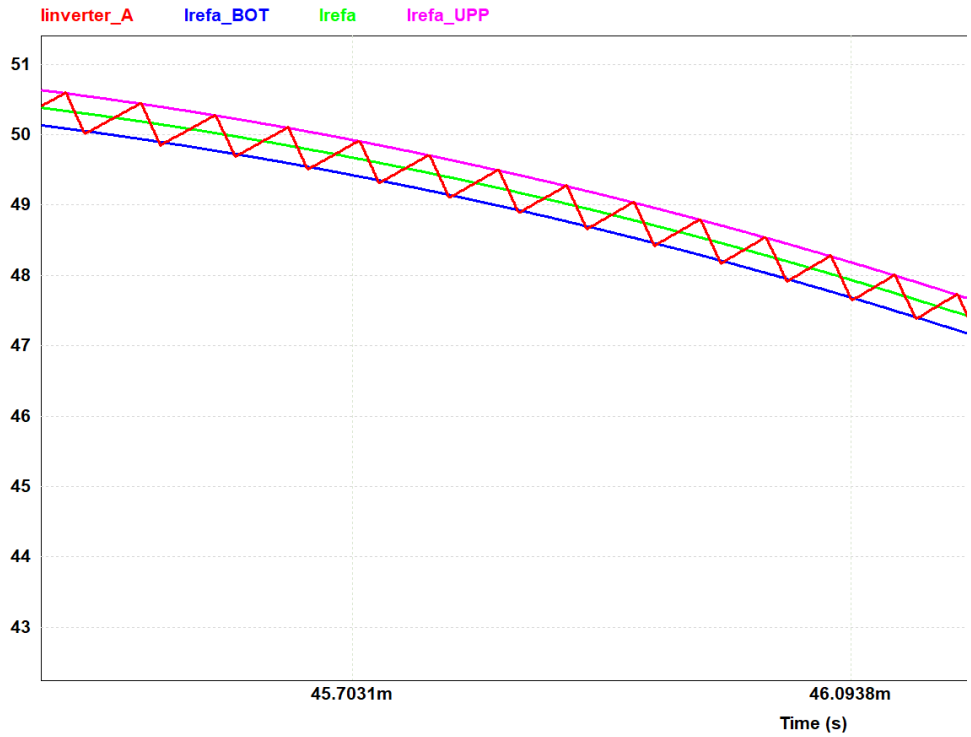

Figure 4.5: hysteresis current controller band

4.4.2. Case 1 Simulation Results: Strong grid-network system (without a filter)

The simulation results of the solar PV system connected to a strong grid network with a 1 mH source impedance will be discussed. Figures 4.5 to 4.8 shows the simulation results before the proposed filter was connected to the system. The purpose is to clearly see the grid current waveform distortion so that they can be compared when the filter is installed. The waveforms of the grid currents indicate distortion caused by both the solar PV system and the non-linear loads. This has led to a %THDi of 41.6%, across the three line currents, as shown in Figure 4.5 and Table 4.3. Figure 4.6 shows the harmonic spectrum of the grid currents, with 3rd and 5^{th} order harmonics being the dominants.

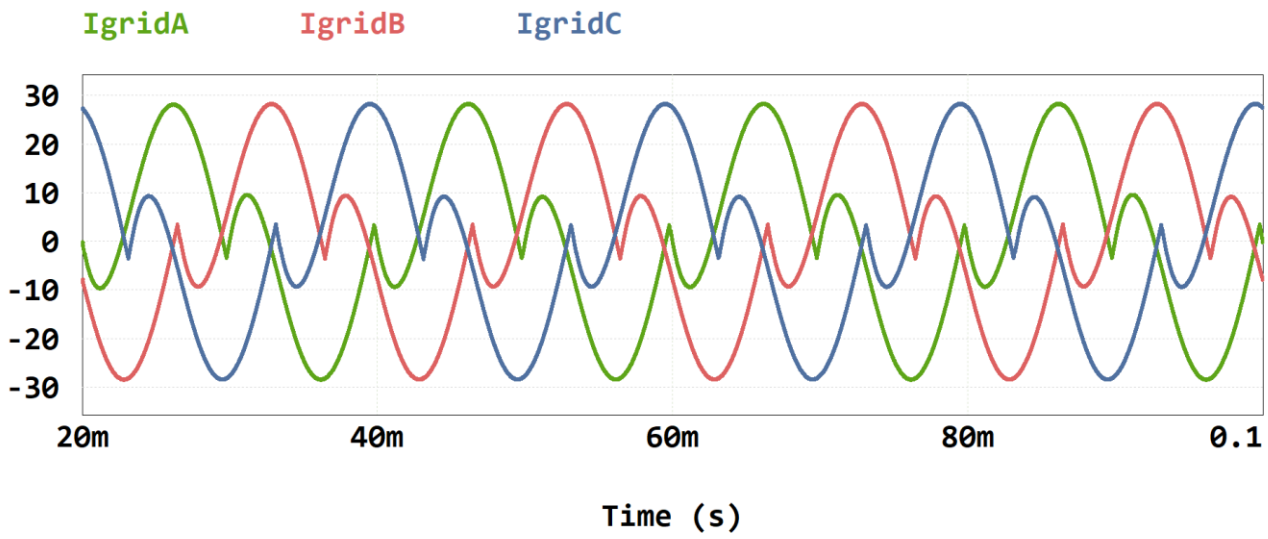

Figure 4.6: Grid currents waveforms when filter not connected in a strong network

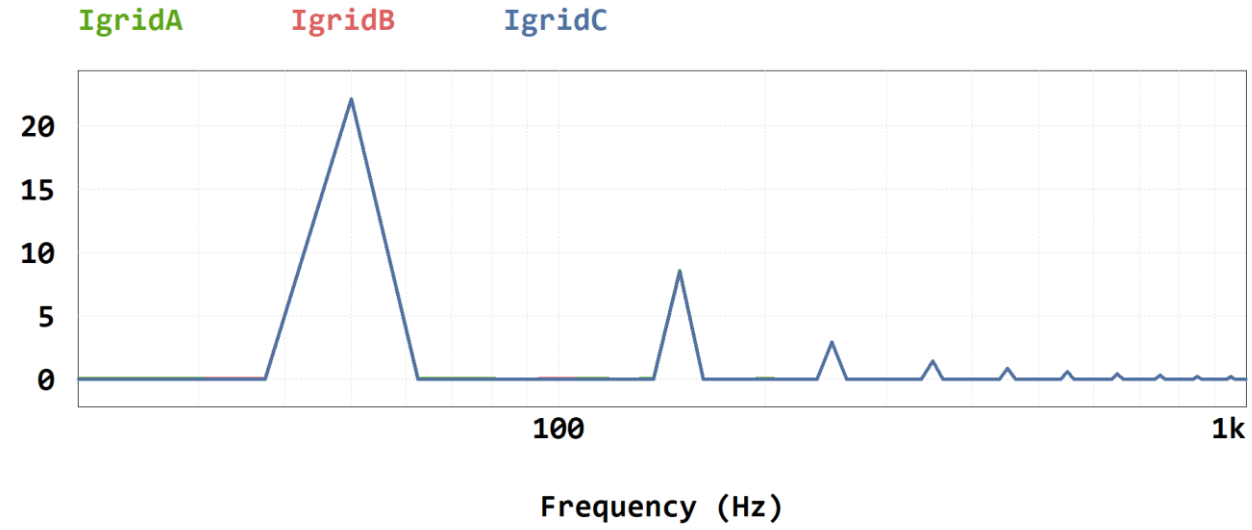

Figure 4.7: Harmonic spectrum of grid current when filter not connected in a strong network

Table 4.3: Total harmonic distortion of grid currents when filter not connected in a strong network

	X1	X2	Δ	THD
Time	6.00002e-02	8.00002e-02	2.00000e-02	freq=50
IgridA	6.06059e-02	-6.24456e-03	-6.68505e-02	4.16695e-01
IgridB	-7.77755e+00	-7.82389e+00	-4.63409e-02	4.14991e-01
IgridC	2.75693e+01	2.75789e+01	9.57326e-03	4.15111e-01

The waveforms of the grid voltages before the connection of the filter are shown in Figure 4.7. The waveforms reveal that both the solar PV system and the non-linear load have distorted the voltage waveforms to a %THDv of 10% as shown in Table 4.4. Figure 4.8 shows that the 3rd (150 Hz) and 5th (250 Hz) order harmonics are the dominant ones in THDv.

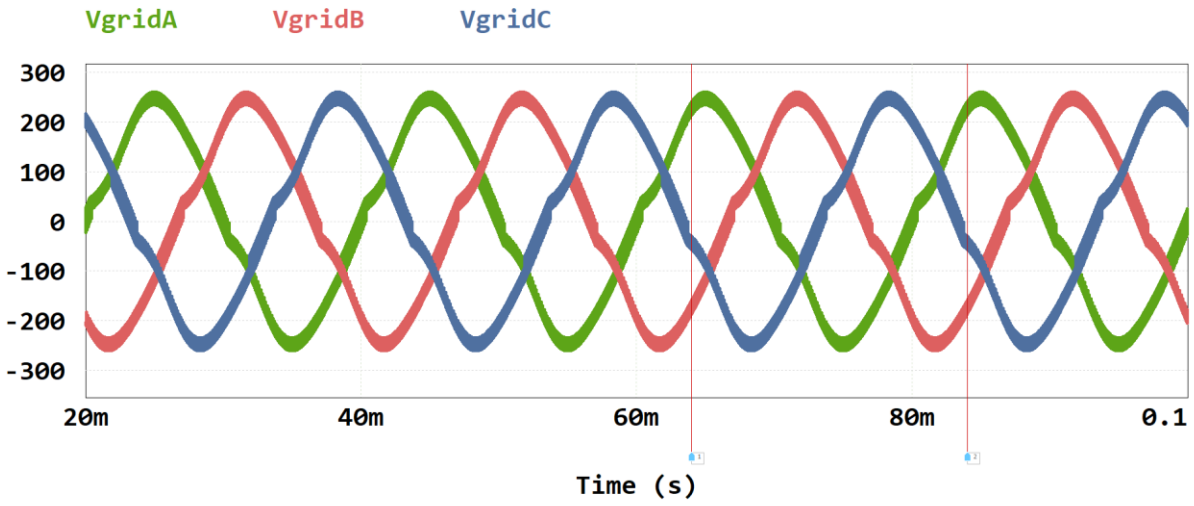

Figure 4.8: Grid voltage waveforms when filter not connected in a strong network

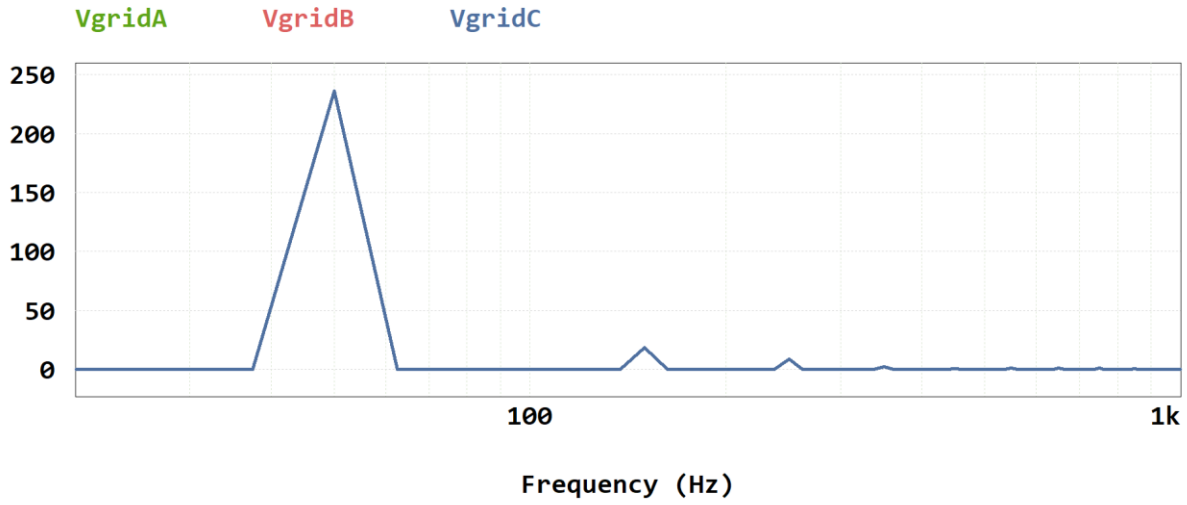

Figure 4.9: Harmonic spectrum of grid voltage when filter not connected in a strong network

Table 4.4: Total harmonic distortion of grid voltage when filter not connected in a strong network

	X1	X2	Δ	THD
Time	6.00002e-02	8.00002e-02	2.00000e-02	freq=50
VgridA	2.51606e+01	-2.24234e+01	-4.75839e+01	1.00914e-01
VgridB	-2.79290e+02	-2.79288e+02	1.31236e-03	1.00941e-01
VgridC	3.04612e+02	2.80237e+02	-2.43747e+01	1.00830e-01

4.4.3. Case 1 Simulation Results: Strong grid-network system (with a proposed filter)

In order to protect the grid network from the identified dominant harmonics, a designed passive RLC filter has been connected to reduce the THD for both voltage and current waveform. Positive results have been achieved when the RLC passive filter was switched ON. The dominant harmonics are not injected into the grid; they are trapped in the RLC passive filter. The 3rd and 5th harmonics are drastically reduced on the grid side, as shown in Figures 4.9 to 4.12 and Tables 4.5 to 4.6. It can be seen that the THDi has been reduced from 41.6% to 2.7%. Through FFT, the harmonic spectrum (Fig. 4.10) shows clearly that the dominant harmonic current components, 3rd and 5th (150 and 250 Hz), have been mitigated. For the grid voltage

waveforms, the distortion of the waveforms was recorded to have a %THDv of 10% before the RLC filter was included. After connecting the tuned RLC filter, the voltage waveform distortion was reduced to 3.7%, as shown in Figure 4.11 and Table 4.6. The dominant harmonic order voltage components were successfully mitigated to protect the grid network.

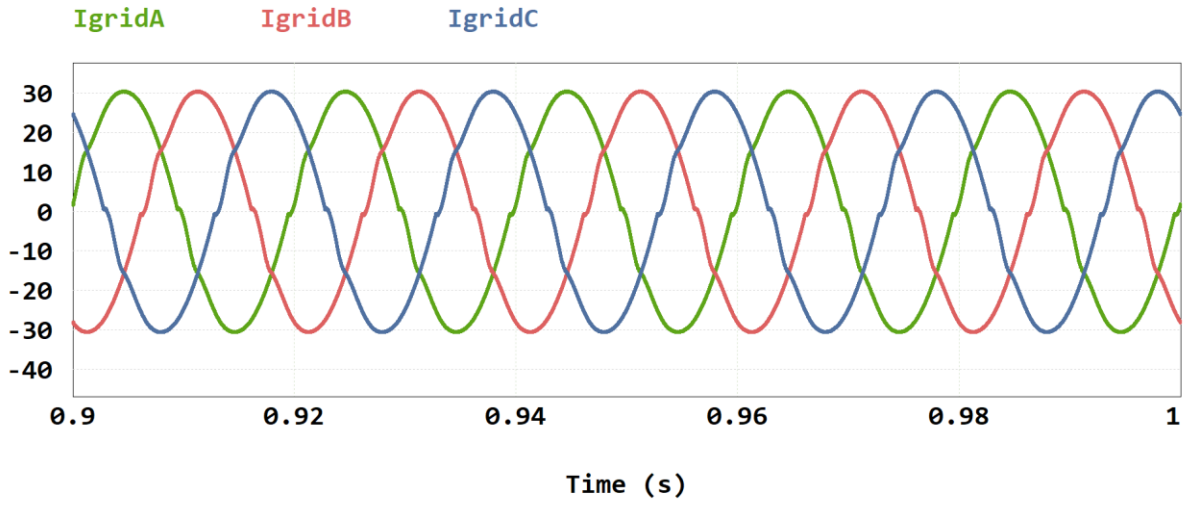

Figure 4.10: Grid currents waveforms when the filter is connected in a strong network

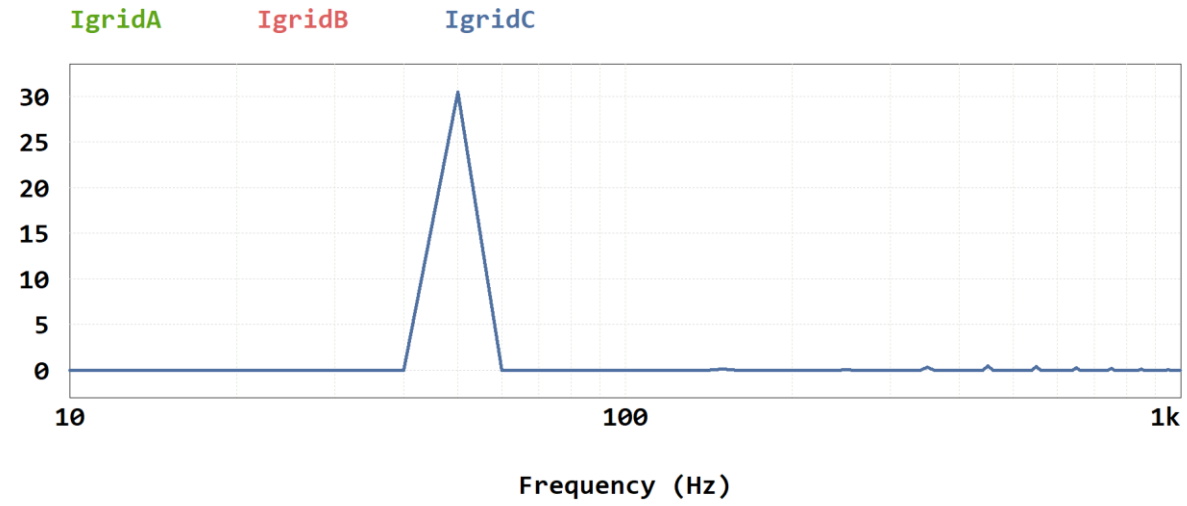

Figure 4.11: Harmonic spectrum of grid current when filter is connected in a strong network

Table 4.5: Total harmonic distortion of grid current when filter is connected in a strong network

Measure

	X1	X2	Δ	Average |X|	THD
Time	9.05000e-01	9.25000e-01	2.00000e-02		freq=50
IgridA	3.02695e+01	3.02570e+01	-1.24837e-02	1.93228e+01	2.70694e-02
IgridB	-1.21957e+01	-1.22154e+01	-1.97108e-02	1.93202e+01	2.71633e-02
IgridC	-1.75351e+01	-1.75376e+01	-2.45378e-03	1.93305e+01	2.70300e-02

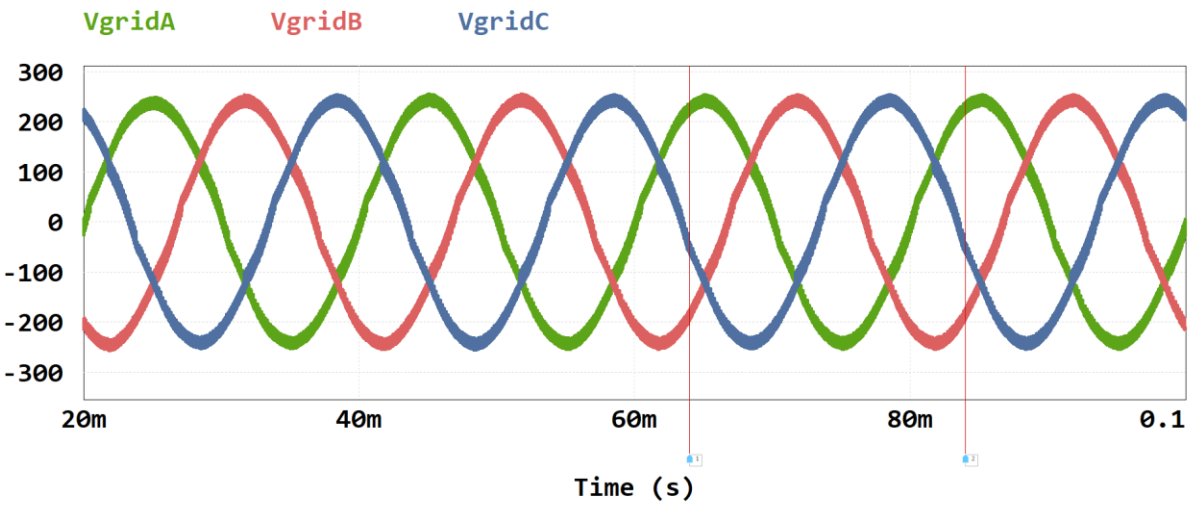

Figure 4.12: Grid voltage waveforms when filter is connected in a strong network

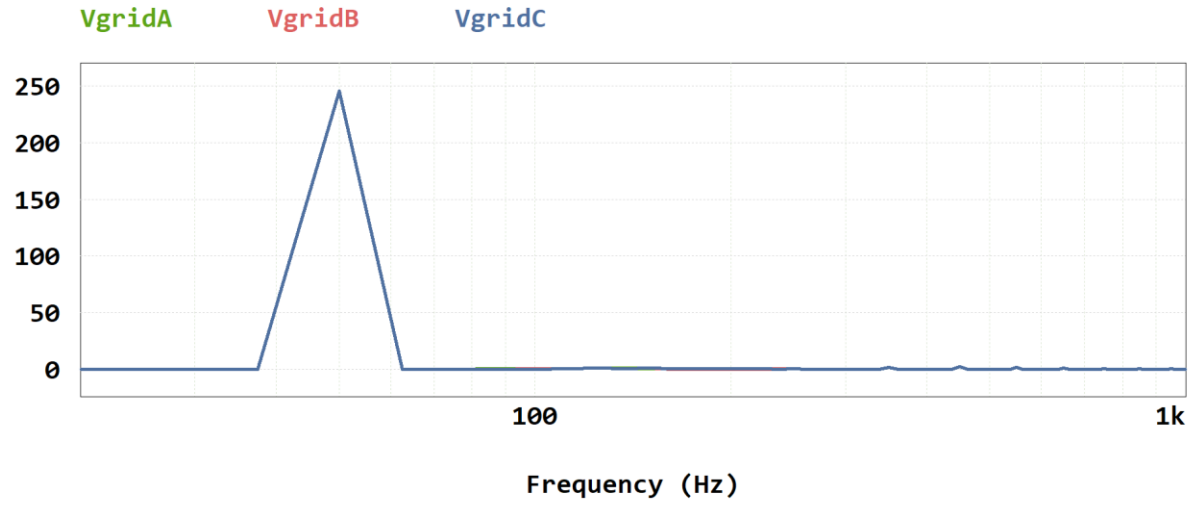

Figure 4.13: Harmonic spectrum of grid voltage when filter is connected in a strong network

Table 4.6: Total harmonic distortion of grid voltage when filter is connected in a strong network

Measure

	X1	X2	Δ	THD
Time	6.00002e-02	8.00002e-02	2.00000e-02	freq=50
VgridA	-4.33184e+00	-4.34442e+00	-1.25735e-02	3.71718e-02
VgridB	-2.95896e+02	-2.96217e+02	-3.20861e-01	3.69161e-02
VgridC	2.95199e+02	3.12003e+02	1.68040e+01	3.70816e-02

4.4.4. Case 2 Simulation Results: Weak grid-network system (without a filter)

In this section, the simulation results of the modelled grid-connected solar PV system have been covered, when the RLC filter is connected and when it is not connected on the system. The source impedance of the grid network has been set to 10 mH to represent a weak grid network. Figures 4.13 to 4.16 show the simulation results before the proposed filter was connected to the system. Figures 13 and 14 illustrate that the three-phase current waveforms (IgridA, IgridB, and IgridC) exhibit a significant distortion level of around 91.4% compared to 41.6% found in the strong grid network scenario (Section 4.4.2). Figure 4.6 shows the harmonic spectrum of the grid currents with 3rd, 5th and 7th order harmonics being the dominants. Similarly, the %THD for the voltage waveforms has increased to a significantly high value of around 38% compared to 10% found in the strong grid network, as shown in Figure 4.15 and Table 4.8. The odd-order harmonics proved to be the dominant ones. This proves that the network impedance plays a part in determining the THD of the system. Hence, it is important to evaluate the grid network impedance before designing a filter for a grid-tied solar PV system.

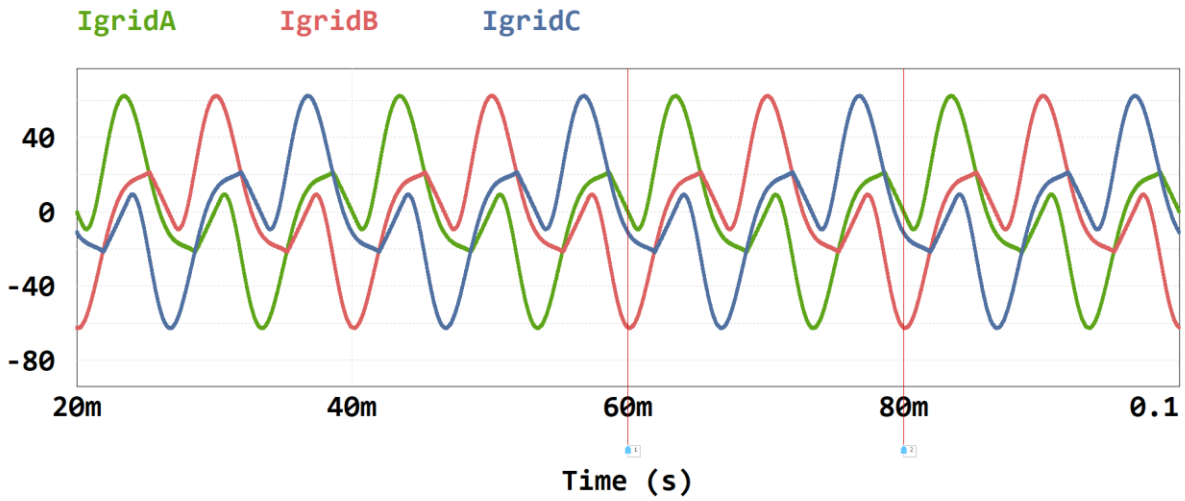

Figure 4.14: Grid currents waveforms when filter not connected in a weak grid-network

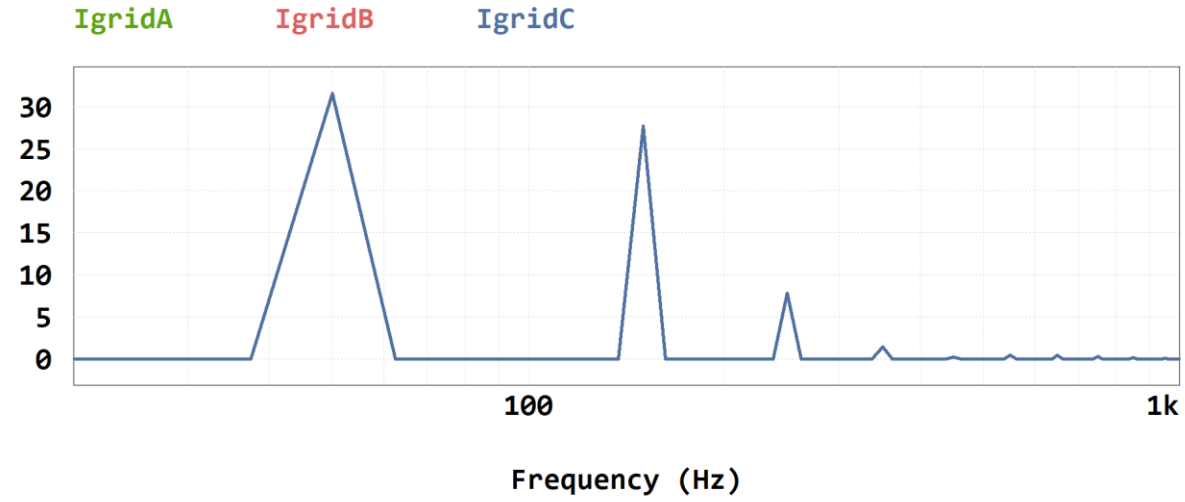

Figure 4.15: Harmonic spectrum of grid current when filter not connected in a weak network

Table 4.7: Total harmonic distortion of grid currents when filter not connected in a strong network

Measure

	X1	X2	Δ	THD
Time	6.00002e-02	8.00002e-02	2.00000e-02	freq=50
IgridA	-5.12536e-02	-1.78809e-01	-1.27555e-01	9.14517e-01
IgridB	-6.20607e+01	-6.22941e+01	-2.33334e-01	9.14240e-01
IgridC	-1.12033e+01	-1.12136e+01	-1.03191e-02	9.14240e-01

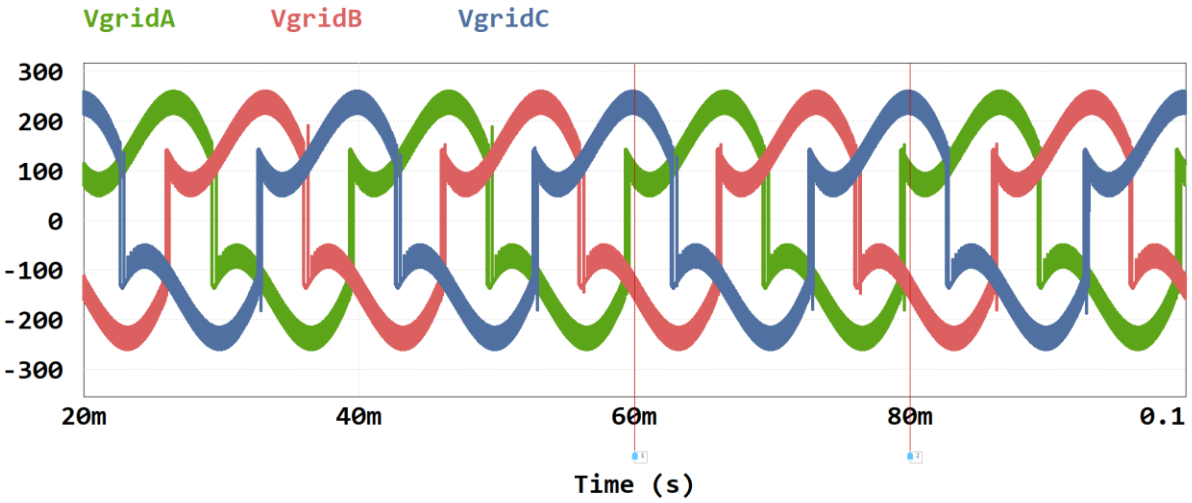

Figure 4.16: Grid voltage waveforms when filter not connected in a weak network

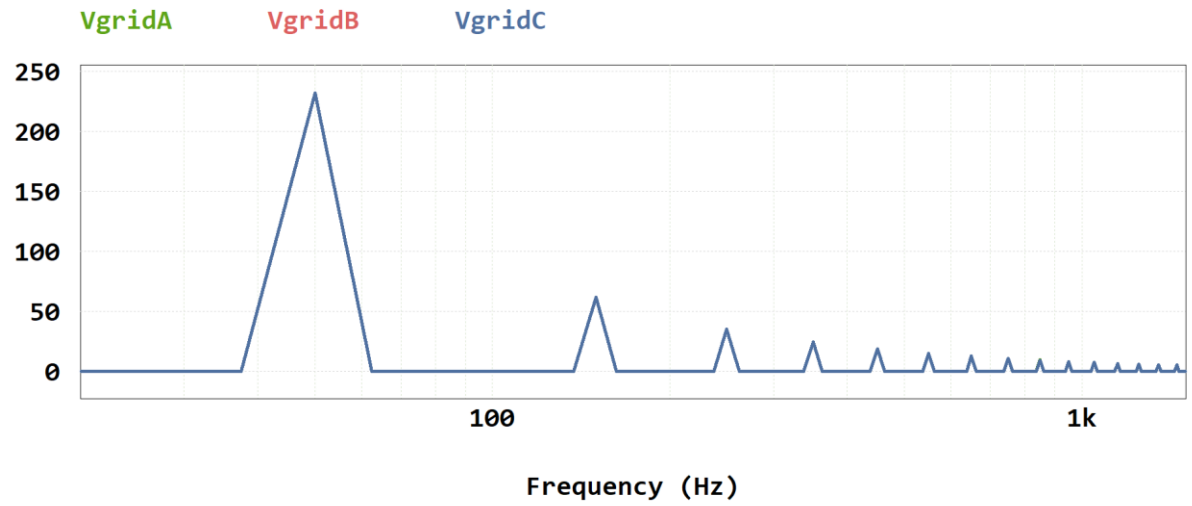

Figure 4.17: Harmonic spectrum of grid voltage when filter not connected in a weak network

Table 4.8: Total harmonic distortion of grid voltage when filter not connected in a weak network

Measure

	X1	X2	Δ	THD
Time	6.00002e-02	8.00002e-02	2.00000e-02	freq=50
VgridA	1.72914e+02	1.73032e+02	1.18254e-01	3.81800e-01
VgridB	-1.72088e+02	-1.72288e+02	-2.00043e-01	3.80672e-01
VgridC	3.28794e+02	3.28780e+02	-1.40970e-02	3.80073e-01

4.4.5. Case 2 Simulation Results: Weak grid-network system (with a filter)

The investigation conducted on the strong grid network was also performed for the weak grid network using the same RLC filter parameters. The filter performed very well for both strong and weak grid networks. Both the voltage and the current waveforms for the weak grid were seen to be severely distorted. The dominant harmonics needed to be trapped using the designed RLC passive filter. By applying the filter, it can be seen that the THDi has been reduced from 91.4% to 3.7%, as shown in Figure 4.17 and Table 4.8. Hence, the harmonic spectrum (Fig. 4.18) shows clearly that the dominant harmonic current components have been mitigated/reduced. For the grid voltage waveforms, the %THD of waveforms has been reduced from 38% to around 5.7% using the filter, as shown in Figure 4.19 and Table 4.9. Hence, dominant-order harmonic voltage components were successfully mitigated to protect the grid network, as shown in Figure 4.20.

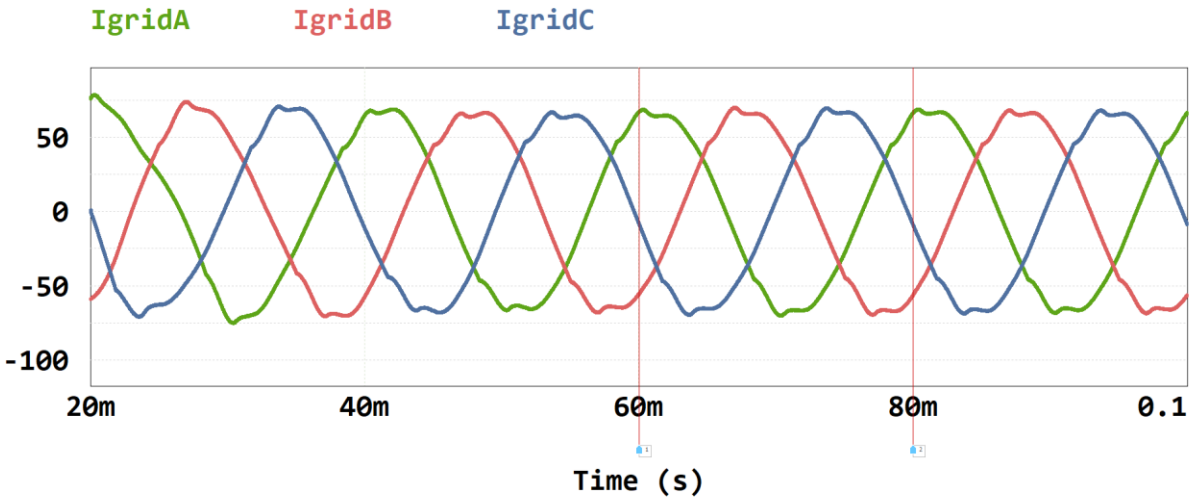

Figure 4.18: Grid currents waveforms when filter is connected in a weak network

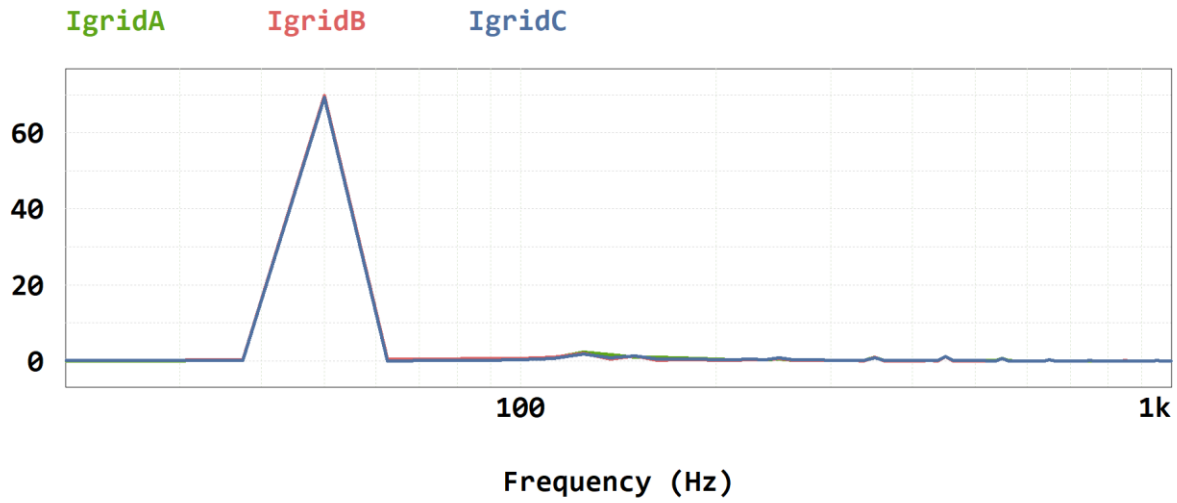

Figure 4.19: Harmonic spectrum of grid current when filter is connected in a weak network

Table 4.5: Total harmonic distortion of grid currents when filter is connected in a strong network

Measure

	X1	X2	Δ	THD
Time	6.00002e-02	8.00002e-02	2.00000e-02	freq=50
IgridA	6.71472e+01	6.66813e+01	-4.65868e-01	3.65096e-02
IgridB	-5.55700e+01	-5.60636e+01	-4.93596e-01	3.46230e-02
IgridC	-7.82439e+00	-8.63722e+00	-8.12826e-01	3.50912e-02

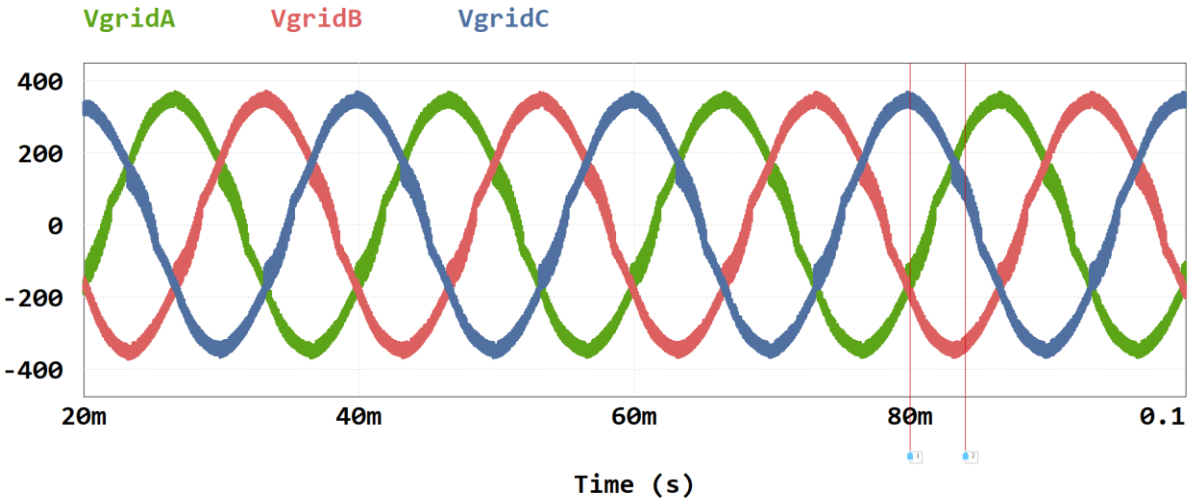

Figure 4.20: Grid voltage waveforms when filter is connected in a weak network

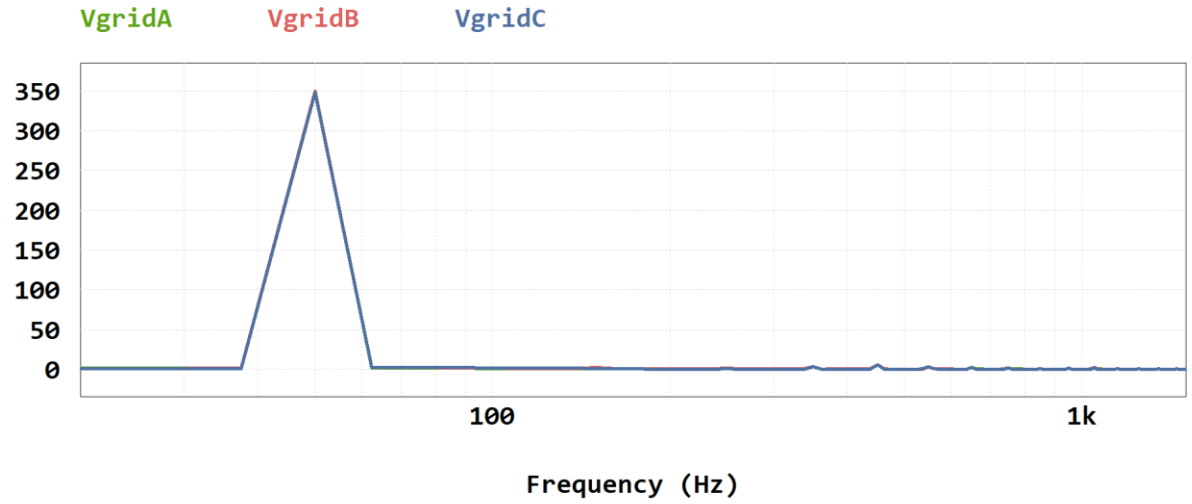

Figure 4.21: Harmonic spectrum of grid voltage when filter is connected in a weak network

Table 4.6: Total harmonic distortion of grid voltages when filter is connected in a weak network

Measure

	X1	X2	Δ	THD
Time	6.00002e-02	8.00002e-02	2.00000e-02	freq=50
VgridA	-2.46956e+02	-2.71643e+02	-2.46871e+01	5.75557e-02
VgridB	-1.94559e+02	-1.99958e+02	-5.39907e+00	5.65687e-02
VgridC	4.31786e+02	4.55081e+02	2.32942e+01	5.72480e-02

CHAPTER 5: CONCLUSION AND FUTURE STUDIES RECOMENDATION

The tuned RLC passive filter has achieved excellent results in both scenarios, in the strong grid and the weak grid. In the strong grid, it drastically reduced the current and voltage waveform distortion from 41,7 % to 2,7 % and from 10% to 3,7% THD, respectively. In the weak grid, it drastically reduced the current and voltage waveform distortion from 91,5% to 3,6% and from 38% to 5,7% THD, respectively. The FFT has clearly shown the reduction of dominant harmonics (3rd and 5th) when the filter was installed. The harmonic content was reduced to fall within the allowable limits according to the NRS standards so that clients are not penalised for injecting the harmonics into the grid. Table 5.1 shows the quantitative highlights of the results achieved.

Scenario	**Filter Status**	**THDi (%)**	**THDv (%)**	**Dominant Harmonics**
Strong Grid Network	Without Filter	41.6	10	3rd, 5th
Strong Grid Network	With Filter	2.7	3.7	Effectively Mitigated
Weak Grid Network	Without Filter	91.4	38	3rd, 5th, 7th
Weak Grid Network	With Filter	3.7	5.7	Effectively Mitigated

Table 5. 1 Comparison of harmonic distortion before and after filtering

The effect of source impedance on harmonic content obtained on the waveforms was noted; the higher the source impedance, the higher the harmonic distortion on the waveform. This applies in both current waveform and voltage waveform.

More studies can be conducted on passive filters, whereby the performance of the filter can be analysed for different phase loading (imbalance phases). The other studies can also be conducted to investigate how the harmonics can further be reduced to close to zero percent in a grid-tied system.

REFERENCES

[1] M. K. Ratshomo, “THE SOUTH AFRICAN ENERGY SECTOR REPORT 2021,” Department of Mineral Resources & Energy, Pretoria, 2021.

[2] M.-L. Van Der Walt, J. Van Den Berg and M. Cameron, “State of Renewable Energy in South Africa,” Department of Energy, Pretoria, 2018.

[3] C. o. C. Town, “Guidelines for imbedded generation,” City of Cape Town, Cape Town.

[4] Annapoorna Chidurala, Tapan Kumar Saha, N. Mithulananthan and Ramesh C. Bansal, “Harmonic Emissions in Grid Connected PV Systems:A Case Study on a Large Scale Rooftop PV Site,” *2014 IEEE Power & Energy Society General Meeting,* 2014.

[5] M. J. Russell, “The Impact of Mains Impedance on Power Quality,” *IEEE,* 2000.

[6] R. Aljarrah, M. Ayaz, Q. Salem, M. Al-Omary, I. Abuishmais and W. Al-Rousan, “Application of Passive Filters in Power Distribution System with High Share of PV systems and Non-Linear loads,” *International Journal of Renewable Energy Research (IJRER),* vol. 13, no. 1, pp. 401-411, 2023.

[7] S. Adak , H. Cangi and A. S. Yilmaz, “Design of an LLCL type filter for stand-alone PV system's harmonics,” *Journal of Energy System,* vol. 3, no. 1, pp. 36-50, 2019.

[8] M. W. Hussain and M. A. Qureshi, “Analysis and Design of Passive Filters for Power Quality Improvement in 3 phase Grid-Tied PV System,” *International Confrerence on Energy Conservation and Efficiency,* pp. 1-6, 2021.

[9] J. C. Das, Power system harmonics and passive ilter design, United States of America: John Wiley & Sons, 2015.

[10] C. Venkatesh, D. Srikanth Kuma, M. Sydulu and Siva Sarma, “Modelling of Nonlinear Loads and Estimation of Harmonics in Industrial Distribution System,” *Fifteenth National Power Systems Conference (NPSC),* pp. 592-597, 2008.

[11] R. Burch, G. Chang, M. Grady and P. Ribeiro, “Impact of Aggregate Linear Load Modeling on Harmonic Analysis: A Comparison of Common Practice and Analytical Models,” *IEEE TRANSACTIONS ON POWER DELIVERY,* vol. 18, no. 2, 2003.

[12] A. P. Singhal, “tricolite.com,” [Online]. Available: https://www.tricolite.com/pdf/sources-eeffects-harmonics.pdf. [Accessed 14 12 2023].

[13] Udo Siegfriedt and Clemens Brandt, “Solar PV Installation Guidelines,” SAPVIA, Johannesburg, 2017.

[14] Dr C Carter-Brown, M Bello, Dr G Botha, L Drotsche, Dr H Geldenhuys, H Groenewald, V Nundlal, S Sewchurran, R van der Riet and A Whittaker, “GRID INTERCONNECTION OF EMBEDDED GENERATION,” SABS Standards Division, Pretoria, 2014.

[15] S. E. Africa, “Wheeling discussion,” Sustainable Energy Africa, 2020.

[16] V. M. Phap, “Study on Grid Connected Photovoltaic System Using PSIM Program,” *International Journal of Science and Research (IJSR),* 2018.

[17] T. S. Energy, “The Sol Energy,” The Sol Energy, [Online]. Available: https://thesolenergy.co.za/grid-tied-off-grid-system/. [Accessed 15 12 2023].

[18] A. F. N. A. R. E. R. A. T. (ANERT), “TECHNICAL SPECIFICATIONS OF HYBRID SOLAR POWER PLANT,” Department of Power, Government of Kerala, Thiruvananthapuram.

[19] Prostar, “Prostar Solar,” Prostar Solar, [Online]. Available: https://www.prostarsolar.net/article/hybrid-solar-systems.html. [Accessed 23 12 2023].

[20] S. reviews, “Solar reviews,” Solar reviews, [Online]. Available: https://www.solarreviews.com/blog/grid-tied-off-grid-and-hybrid-solar-systems. [Accessed 23 12 2023].

[21] W. Mack Grady and Surya Santoso, “Power System Harmonics,” *IEEE Xplore,* 2001.

[22] Sibulele Mtakati, Peter Freere and Alan Roberts, “Design and Comparison of Four Branch Passive Harmonic Filters in Three Phase Four Wire Systems,” *2019 IEEE AFRICON,* 2020.

[23] Niharika Singh, N K Sharma' and P Tiwari, “Harmonics: Sources, Effects and Control Techniques,” *NIET Journal of Engineering & Technology,,* vol. 1, no. 1, 2012.

[24] I. S. Association, “IEEE Recommended Practice and Requirements for Harmonic Control in Electric Power Systems,” *IEEE,* 2014.

[25] Nweke F. U., “Strategies for Eliminating Harmonics in an Inverter AC Power Supply,” *IOSR Journal of Electrical and Electronics Engineering (IOSR-JEEE) ,* vol. 10, no. 4, pp. 2320-3331, 2015.

[26] M. Sharma, A. Achra, V. Gali and M. Gupta, “Design and performance analysis of interleaved inverter topology for photovoltaic applications,” *International Seminar on Application for Technology of Information and Communication,* vol. 1, no. 6, pp. 14-27, 2021.

[27] S. N. Haq, A. S. Budi and F. A. Pamuji, “Photovoltaic Sudden Cloud Compensation Devise Using Modified LCL Filter Converter Configuration,” *International Seminar on Application for Technology of Information and Communication,* pp. 365-369, 2021.

[28] S. Adak and H. Cangi, “Elimination of harmonic components in solar system with L and LC passive filters,” *International Journal of Energy and Smart Grid,* no. 6, pp. 14-27, 2021.

[29] A. Aljwary, Z. Yusupov, Shokirov and O. Toirov, “Mitigation of load side harmonic distortion in standalone photovoltaic based microgrid,” *E3S Web of Conference,* vol. 304, p. 01010, 2021.

[30] S. Adak , “Harmonics mitigation of stand-alone photovoltaic system using LC passive filter,” *Journal of Electrical Engineering & Technology,* vol. 5, no. 16, pp. 2389-2396, 2021.

[31] S. Dlamini , I. E. Davidson and A. A. Adebiyi, “Application of the passive filters for improved power quality in stand-alone OV systems,” *South African Unviversities Power Engineering Conference (SAUPEC),* pp. 1-6, 2023.

[32] M. R. Dua and M. A. Agrawal, “Impact of single tuned filter on grid connected PV system,” *METHODOLOGY,* no. 8, 2019.

[33] R. A. Raj, T. Aditya and M. R. Shinde, “Power Quality enhancement of grid-connected solar photovoltaic system using LCL filter,” *International conference on Power Electronics & IoT Applications in Renewable Energy and its Control (PARC),* pp. 334-339, 2020.

[34] L. Gumilar, D. E. Cahyani, A. N. Afandi, D. Monika and S. N. Rumokoy, “. Optimalization harmonic shunt passive filter using detuned reactor and capacitor bank to improvement power quality in hybrid power plant,” *AIP Conference Proceedings,* vol. 2217, no. 1.

[35] L. Muhammad, W. Lei, M. A. Amin, W. D. Feng and M. T. Faiz, “Parameter designing method of active damping LCL filter for grid-connected inverter.,” *International Multitopic Conference (INMIC),* pp. 1-6, 2020.

[36] L. Xiong, M. Nour and E. Radwan, “Harmonic analysis of photovoltaic generation in distribution network and design of adaptive filter,” *International Journal of Computing and Digital Systems,* vol. 1, no. 9, 2020.

[37] X. Shi and H. T. Le , “Mitigating Harmonics from Residential Solar Photovoltaic Systems,” *IEEE PES Innovative Smart Grid Technologies-Asia (ISGT Asia),* pp. 1-5, 2021.

[38] S. Khalil S, N. Oumidou, M. Lhayani and M. Cherkaoui, “Connection of a passive filter in parallel for harmonic compensation in a grid-connected PV System,” *Engineering for Smart and Sustainable Systems Research Center,* 2021.

[39] R. Moyal and D. Shivam, “Harmonic Mitigation in Modelled Grid Connecting Solar Photovoltaic Array System in MATLAB,” *Indian International Conference on Industrial Engineering and Operations Management Warangal, Telangana, India,* pp. 16-18, 2022.

[40] Zhong F, Chang G W and K. T. Nguyen , “A new damping scheme of llcl filter for grid-tied pv inverter output harmonics mitigation,” *International Conference on harmonics & Quality of Power (ICHQP),* pp. 1-6, 2020.

[41] Y. Al-Sharif, G. Sowilam and T. Kawady, “Harmonic Analysis of Large Grid-Connected PV Systems in Distribution Networks: A Saudi Case Study,” *International Journal of Photoenergy,* vol. 1, p. 8821192, 2022.

[42] M. Hosseinpour and A. Kholousi, “. Design and Analysis of LCL-type Grid-Connected PV Power Conditioning System Based on Positive Virtual Impedance Capacitor-Current Feedback Active Damping,” *Journal of Solar Energy Research,* pp. 1497-1515, 2023.

[43] N. F. Ibraham , M. M. Mahmoud, A. M. Al Thaiban, A. B. Barnawi, Z. S. Elbarbary, A. L. Omar and H. Abdelfattah, “. Operation of grid-connected PV system with ANN-based MPPT and an optimized LCL filter using GRG algorithm for enhanced power quality,” *IEEE Access,* 2023.

[44] S. Khalil, N. Oumidou and M. Cherkaoui, “Compensation of Current Harmonic Distortion in a Grid-Connected Photovoltaic System via an LC Filter,” *International Conference on Digital Technologies and Applications,* pp. 632-642, 2023.

[45] Y. Djeghader, S. Boumous and Z. Boumous, “Study and analysis of the propagation of harmonics in electrical grid connected photovoltaic system,” *Diagnostyka,* no. 24, 2023.

[46] R. Aljarrah, M. S. Ayaz, Q. Salem, M. AL-Omary, I. Abuishmais and W. Al-Rousan, “Application of Passive Harmonic Filters in Power Distribution System with High Share of PV Systems and Non-Linear Loads,” *International Journal of Renewable Energy Research(IJRER),* vol. 1, no. 13, pp. 401-411, 2023.

[47] R. Ingale, “Harmonic Analysis Using FFT and STFT,” *International Journal of Signal Processing,* vol. 7, pp. 345-362, 2014.

[48] S.-R. Marwa Ben, W. N. Mohamed, B. Ilhem Slama and M. Eric, “An Improved LCL Filter Design in Order to EnsureStability without Damping and Despite Large Grid Impedance Variations,” *Energies,* vol. 10, pp. 1-19, 2017.

[49] L. C, W. M, C. W, X. Cui, M. Mei and Z. Liu, “Design and Performance of an Adaptive Low-DC-Voltage-Controlled LC-Hybrid Active Power Filter With a Neutral Inductor in Three-PhaseFour-Wire Power Systems,” *IEEE TRANSACTIONS ON INDUSTRIAL ELECTRONICS,* vol. 61, no. 6, 2014.

[50] R.-P. ´. e. Javier, A.-M. ´. ´. Regulo, R.-C. Alberto , P. Milan and B. Emilio, “LTCL-Filter Active-Damping Design Considerations for Low-Switching-Frequency Grid-Tied VSCs,” *IECON 2018-44th Annual Conference of the IEEE Industrial Electronics Society ,* pp. 1315-1320, 2018.

[51] P. I, I. C, A. L, L. A, R. T and F. B, “Current Harmonics Cancellation in Three-Phase Four-Wire Systems by Using a Four-Branch Star Filtering Topology,” *IEEE TRANSACTIONS ON POWER ELECTRONICS,* vol. 24, no. 8, 2009.

[52] S. A. W. E. Association, “The cost benefits of renewable energy,” SAWEA, 2019.

[53] H. A. Smadi, “Overview of Grid-Connected PV Systems Challenges with Regards to Grid Stability,” *Research Gate,* 2018.

[54] H. T. Henning X and P. Dr. Tomaz, “Hybrid Filter for Dynamic Harmonics Filtering and Reduction of Commutation Notches”.

[55] P. A. Gbadega and S. K. Akshay , “Comparative study of Harmonics Reduction and Power Factor enhancement of Six and 12-pulses HVDC system using passive and shunt APFs Harmonic Filters”.

[56] S. Rahmani, Ab. Hamad, K. Al-Haddad and H. Y. Kanaan, “A Multifunctional Power Flow Controller for Photovoltaic Generation Systems with Compliance to Power Quality Standards,” pp. 894-903, 2012.

[57] “Hybrid Filter for Dynamic Harmonics Filtering and Reduction of Commutation Notches”.

[58] Bhim , Singh; Shailendra , Kumar, “Distributed Incremental Adaptive Filter Controlled Grid Interactive Residential Photovoltaic-Battery Based Microgrid for Rural Electrification,” 2020.

[59] Rajan Kumar, Asit Mohanty, S.R.Mohanty and Nand Kishor, “Power Quality Improvement in 3-Φ Grid Connected Photovoltaic System with Battery Storage,” 2012.

[60] Anne Ko, Wunna Swe and Aung Zeya, “Analysis of Harmonic Distortion in Non-linear Loads,” *The First International Conference on Interdisciplinary Research and Development,* 2011.

[61] D. M. Soomro and M. M. Almelian, “OPTIMAL DESIGN OF A SINGLE TUNED PASSIVE FILTER TO MITIGATE HARMONICS IN POWER FREQUENCY,” *ARPN Journal of Engineering and Applied Sciences,* vol. 10, no. 19, pp. 909-9014, 2015.